X-RAY IRRADIATION EFFECTS ON THE Mo(V)-Mo(VI) SYSTEM IN AQUEOUS MEDIA

by

DONALD FREDERICK PADDLEFORD

B. S., Kansas State University, 1960

A MASTER'S THESIS

submitted in partial fulfillment of the

requirements for the degree

MASTER OF SCIENCE

Department of Nuclear Engineering

KANSAS STATE UNIVERSITY
Manhattan, Kansas

1962

TABLE OF CONTENTS

TABLE OF CONTENTS (concl.)

NOMENCLATURE

A - sample absorbance ($\log_{10} I_0/I$).

a_i - constants appearing in spectrophotometry study.

C - concentration.

$C_i(\underline{r},t)$ - probability density of finding a particle of species x_i at a position determined by $\underline{r}$ at a time t after the onset of the chemical stage.

D_i - diffusion coefficient of x_i.

E - energy.

G - ions changed per 100ev. absorbed energy.

I - intensity of light transmitted by sample.

I_0 - intensity of light incident on sample.

J - ionization produced per unit mass in air.

k_i - reaction rate constant.

K_i - constants in absorbance equation.

K.V. - kilovolts.

M - mass.

$m\mu$ - millimicron.

ma - milliampere.

N - normality, gm-moles/liter.

n - total number of reactive species.

pH - minus the $\log_{10}$ of the hydrogen ion concentration.

q - total number of unreactive species.

$\underline{r}$ - position vector, $d\underline{r}$ is an infinitesimal volume element.

S_m - ratio of mass stopping power of the solution to that of air.

t - time after onset of chemical stage.

NOMENCLATURE (cont.)

W - the absorbed radiation energy required to form an ion pair in air, 32.5ev.

x_i - the species present in solution.

Greek letters.

δ_{ij} - Kronecker delta.

∇^2 - three dimensional Laplacian operator.

λ - wavelength of light, mμ.

μ - micron, 10^{-6} M.

INTRODUCTION

Background Information

Many experimental studies have been made on basic compounds and solutions, which have contributed greatly to the understanding and prediction of radiation effects on materials. The experimental effects of irradiation on some materials have been established to the extent that they are being used to determine the quality and to measure the quantity of radiation.

The theories and reaction mechanisms proposed for the effects of radiation on these basic systems are in a state of gradual refinement. Evidence for a number of mechanisms proposed for these basic systems is continually being substantiated.

In the area of aqueous solutions of inorganic compounds, the ground work of the reaction mechanisms has been laid. Certain underlying theories have been developed and investigated to the extent that they are being taken as correct. Several systems of inorganic salts in water media have been found to undergo oxidation or reduction reactions when exposed to ionizing radiation. Gold and silver salts are reduced to the metals by x-rays in the presence of molecular hydrogen in solution (27). Mercuric ions from soluble mercuric chloride are precipitated out of solutions exposed to x-ray irradiation as mercurous chloride (28). X-rays reduce ceric ions to cerous ions (9). Irradiation, by x-rays, of solutions of ferrous or cuprous ions causes the oxidation reaction to ferric (22) and cupric ions.

The ferrous-ferric system is reversible in that oxidation or reduction can take place depending on such parameters as atmosphere surrounding the solution and pH.

The amount of oxidation or reduction occurring has been found to be dependent on such parameters as the type and intensity of the radiation, the total absorbed dose, the concentration of other electrolytes present, the presence of dissolved gases, and the atmosphere of the sample being irradiated.

In recent years there has been the development of a diffusion kinetic model (3), (4), (5), (6), (7), (14), (16), (17), (23), (25) to explain the results observed. This model involves the reaction rate constants and the diffusion constants of all species taking active part in the reaction. It requires some physical approximations concerning the amount, energies, and positions of the ions and electrons produced by the radiation. Basically it is assumed that the free radicals, H, OH, and HO_2, are produced and diffuse through the medium to react with the reactive species present. The reactions are of very short order time and the high concentration gradients require that the reaction rate and diffusion constants be time dependent.

At the present time, approximations of only the order of magnitude of the reaction rate and diffusion constants can be made thus limiting the model to very approximate results. Further, due to the multiplicity of parameters, it is always possible to adjust them to make the model give results in

agreement with experimental observations as has been noted by some investigators (15).

Statement of Problem

The objective of this investigation was to study the effect of x-ray radiation on the Mo(V)-Mo(VI) system. X-ray irradiation was applied to molybdenum ions to investigate whether or not any oxidation or reduction takes place. In the well investigated ferrous-ferric and ceric-cerous systems, the radiation effect has been found to depend on several parameters. Over certain ranges of concentration, pH, total dose, and dose rate, the number of ions in the solution that are oxidized or reduced is proportional to the absorbed dose. The proportionality can be expressed in terms of the G value which is defined as the number of ions changed per 100 ev. of absorbed radiation energy. Once the G value is established, the system is a potential method of measuring radiation dose.

It was the purpose of this investigation to find the G value of the molybdenum system, providing that an oxidation or reduction change takes place. The G value was measured experimentally over various ranges of the above mentioned parameters. As the oxidation or reduction changes of ionizing radiation are very slight, a sensitive method of analysis was needed. Several analytical procedures for determining the molybdenum ion concentration were investigated. Should the G value of the molybdenum system be found constant over a

reasonable range of the parameters under investigation and should the method of analysis of the irradiated solution be rapid and accurate, the molybdenum ion reaction to x-ray irradiation could be used as a radiation dosimeter.

THEORETICAL

Diffusion Kinetic Theory

Kuperman and Belford (14) have published a rather complete treatise on the diffusion kinetic theory in radiation chemistry. This section summarizes their views.

Absorption of energy from radiation by matter produces a variety of excited species, such as excited molecules in their ground or electronically excited states. Insofar as the absorption phenomenon is a highly localized one, these species have a highly inhomogeneous spatial distribution and constitute the "tracks" of the radiation. The excited species are energetically unstable and undergo a sequence of transformations which terminate when thermodynamic equilibrium is re-established. The first set of these transformations are stable molecules, some of which differ from those originally present, and chemically unstable species such as free radicals. The next set of transformations consists of diffusion and chemical reactions involving these reactive species and leads to chemical equilibrium.

This process can conveniently be divided into three stages:

a) The physical stage, consisting of the dissipation of radiation energy in the system. Its duration is of the order of 10^{-13} sec. or less.

b) The physiochemical stage, consisting of the processes which lead to the establishment of thermal equilibrium in the system. Its duration is usually of the order of 10^{-11} sec.

c) The chemical stage, consisting of diffusion and chemical reaction of the reactive species, and leading to the establishment of chemical equilibrium. Its duration ranges from 10^{-8} sec. up.

The designation "primary" species is given to all species present at the beginning of the chemical stage. Four categories of species will be considered. Three refer to reactive species and the fourth to non-reactive species. The first category is comprised of the several reactive species already present in the system before it is irradiated. These may include molecules of solvent and of one or more solutes contained in the system. They can react only with species from other categories. The second category contains the primary reactive species produced by the irradiation. The third category includes the secondary reactive species formed as a consequence of reactions involving the primary ones. The fourth category includes all products of the radiation chemical reactions which are not reactive with any species ever present in the system during the chemical stage.

Let x_i represent any kind of species, be it reactive (primary, secondary, reactive solute or solvent) or not. These are differentiated from each other by the following notation:

For $i = 1,2, \ldots, p$ x_i denotes reactive primary species.

For $i = p+1, p+2, \ldots, p+s$ x_i denotes a reactive secondary species.

For $i = p+s+1, p+s+2, \ldots, p+s+u = n$ x_i denotes a reactive solute (scavenger) or the solvent if it is reactive.

For $i = n+1, \ldots, n+q$ x_i denotes a non-reactive species not initially present.

According to this notation, there are $n = p+s+u$ different reactive species and q unreactive species.

Macroscopically, diffusion and reaction rate laws are usually expressed in terms of concentrations (or activities) of the species involved. These concentrations are actually statistical averages of number densities. However, in track effects in the radiation chemistry of water, large changes in the number densities of radicals occur within small volumes, so that the concept of a radical concentration becomes meaningless. For this reason, probability densities are used instead.

Let O be an arbitrary origin of co-ordinates. Let $C_i(\underline{r},t)$ be, by definition, the probability density of finding a particle

of species x_i ($i = 1,2, \ldots ,n+q$) at a position in the system determined by vector $\underline{r}$, at time t after the onset of the chemical stage. C_i can be thought of as a generalized concentration, even when small numbers of particles are considered or when very steep concentration gradients are involved.

It is of interest to consider the normalization properties of the probability densities $C_i(\underline{r},t)$.

Let $$N_i(t) = \int C_i(\underline{r},t)d\underline{r} \qquad (1)$$

where the integral is extended over the total volume of the system. If x_i is a primary or secondary species, or a non-reactive species not initially present, then $N_i(t)$ is the average number of particles of species x_i present in the system at time t. For secondary species, as well as non-reactive species not initially present, $N_i(t)$ vanishes at $t = 0$. If the system is infinite, then $N_i(t)$ would be infinite for solutes homogeneously distributed at $t = 0$ or for the solvent. This makes it convenient not to define $N_i(t)$ for this category of species.

It is assumed that any kind of species can disappear or be formed by any first or second order reaction occurring in the bulk of the system. The reactions can generally be represented by the following:

$$x_i \xrightarrow{k_i} \text{products}. \quad \text{First order disappearance.} \qquad (2)$$

$$x_i + x_j \xrightarrow{k_{ij}} \text{products} \ (j = 1,2, \ldots ,n). \quad \text{Second order disappearance.} \qquad (3)$$

$$x_a \xrightarrow{k_{ai}} x_i + \text{products} \quad (a = 1,2, \ldots ,n). \quad \text{First order appearance} \tag{4}$$

$$x_b + x_d \xrightarrow{k_{bidi}x_i t} x_i + \text{products} \quad (b,d = 1,2, \ldots ,n;\ b,d, \neq i). \quad \text{Second order appearance.} \tag{5}$$

All rate constants above refer to the rate of disappearance of reactants and are permitted to be time dependent. If x_i is not reactive, k_i and k_{ij} vanish. The purpose of including first order reactions is to permit inclusion of reactions involving the solvent and to simplify the diffusion kinetic equations when a scavenger can be considered to diffuse infinitely fast.

The chemical effects of the bombardment of a system by a stream of high energy particles or electromagnetic quanta can, for dose rates that are not high, be pictured as the sum of the separate effects of individual particles or quanta.

In the absence of dose rate effects, it is sufficient to consider the effect of the absorption of energy from a single high energy quantum or particle. The total result is obtained by multiplying the one particle effects by the number of particles whose energy was absorbed.

At the beginning of the chemical stage, the absorption of energy from a single particle or quanta has brought about a certain initial distribution of primary reactive species which is in thermal equilibrium with the medium. These species diffuse and react. The time rate of change of the probability density of x_i at a fixed position $\underline{r}$ of the medium is the

algebraic sum of the effects of the net rate of diffusion of particles x_i to this position and their rates of appearance and disappearance due to reactions occurring at this position. This can be expressed by the equation

$$\partial c_i(\underline{r},t)/\partial t = D_i\nabla^2 c_i - k_1 c_i - \sum_{j=1}^{n} k_{ij} c_i c_j + \sum_{a=1}^{n} k_{ai} c_a$$

$$+ \sum_{b,d=1}^{n} (1 - \tfrac{1}{2}\delta_{bd}) k_{bidi} c_b c_d . \qquad (6)$$

All symbols have been defined, except D_i, which is the diffusion coefficient of x_i; δ_{ij}, which is the usual Kronecker delta ($\delta_{ij} = 1$ for $i = j$ and 0 for $i \neq j$); and ∇^2 which is the usual three dimensional Laplacian operator.

Equation (6) constitutes a set of n simultaneous non-linear partial differential equations which, in general, cannot be solved by analytical integration.

The model may apply to a cylindrical ion track or to a string of spherically symmetrical ion clusters. The initial distribution can vary in the model. On physical grounds a Gaussian distribution with respect to the distance to the axis of the cylindrical track or center of the spherical cluster has been justified by considering the mean displacement of an electron as it moves away from the parent ion, before it becomes attached to a neutral molecule.

When considering the distribution of spherical spurs along the track of a charged particle, one must examine cases of low, intermediate, and high LET (linear energy transfer),

which is the energy lost per unit path length as a particle traverses a medium.

For sufficiently low LET the spurs are sufficiently separated so that they do not interact with each other. For intermediate values of LET the spheres overlap. For high LET the spherical tracks overlap to the degree that the track becomes a cylinder with practically no variations in the initial probability density of species along the axis of the track.

The initial conditions for non-primary species and for secondary species are $C_i(\underline{r},0) = 0$ and $C_i(\underline{r},0)$ = initial concentration for homogeneous solutes and solvent. The boundary conditions for all cases fix the values of C_i at infinite values of the space co-ordinates and at any instant of time. For each primary and secondary species, this probability density is zero, whereas for solute or solvent it is equal to its initial value.

The set of equations is solved by numerical integration using the difference equation approximations after converting the equations (6) to dimensionless equations. At the present time, the diffusion constants and the reaction rate constants are not known in general. This seriously limits the usefulness of equation (6) in determining $C_i(\underline{r},t)$ and thus the radiation yields. For this reason the accepted radiation yields are soley determined experimentally.

Free Radical Effect

The radiation induced decomposition of water is the most thoroughly studied system. The primary phenomenon in the irradiation of water is the formation of the free radicals H and OH (Appendix A).

$$H_2O \xrightarrow{\text{radiation}} H + OH \qquad (7)$$

Free radicals do not have stable electron configurations. For this reason they react in very short times. Their mean life time is in the order of microseconds. Possible reactions of the free radicals are:

$$H + H \text{ ----- } H_2 \qquad (8)$$

$$OH + OH \text{ ----- } H_2O_2 \qquad (9)$$

$$H + OH \text{ ----- } H_2O. \qquad (10)$$

Additional reactions leading to the removal of H_2 and H_2O_2 from the system are:

$$H + H_2O_2 \text{ ----- } H_2O + OH \qquad (11)$$

$$OH + H_2 \text{ ----- } H_2O + H. \qquad (12)$$

Reactions (11) and (12) taken together are chain reactions which re-establish the free radical. Other reactions that can break the chain are:

$$OH + H_2O_2 \text{ ----- } HO_2 + H_2O \qquad (13)$$

$$HO_2 + H \text{ ----- } H_2O_2. \qquad (14)$$

These reactions indicate that OH behaves as an oxidizing agent, while H behaves as a reducing agent (22). Therefore, in the ferrous-ferric system the hydroxyl radical oxidizes the

ferrous ion as such,

$$Fe^{+2} + OH \text{ ----- } Fe^{+3} + OH^{-}, \quad (15)$$

and in the cerous-ceric system the hydrogen atom reduces the ceric ion as such,

$$Ce^{+4} + H \text{ ----- } Ce^{+3} + H^{+}. \quad (16)$$

In any aqueous system, dissolved oxygen promotes further oxidation as shown by the following reactions for the ferrous-ferric system:

$$H + O_2 \text{ ----- } HO_2 \quad (17)$$

$$Fe^{+2} + HO_2 \text{ ----- } Fe^{+3} + HO_2^{-} \quad (18)$$

$$HO_2^{-} + H^{+} \text{ ----- } H_2O_2 \quad (19)$$

$$Fe^{+2} + H_2O_2 \text{ ----- } Fe^{+3} + OH^{-} + OH. \quad (20)$$

Dissolved hydrogen inhibits oxidation and promotes reduction by shifting equilibrium (12) to the right. High acidity, or low pH, favors oxidation as it shifts reaction (19) to the right producing more H_2O_2, an oxidizing agent.

The general radiolysis equation is, therefore,

$$H_2O \text{ ----- } H_2, H_2O_2, H, OH, HO_2. \quad (21)$$

Effect of Different Types of Radiation

The chemical effects produced in irradiated aqueous solutions result from excitation and ionization of the system molecules by the passage of radiation. Many times it is qualitatively and sometimes quantitatively true that all types of radiation produce the same chemical effect when equal energies are dissipated in the material. Considering quanti-

tative aspects, it is convenient to divide nuclear radiation into two groups. Group one consists of the fast, light particles such as betas. Group two consists of the heavy, slow particles including alphas, accelerated protons and deutrons, and fission products at the instant of fission. X- and gamma rays are in group one since they produce their effects through secondary electrons, that is, the photoelectric effect, the compton effect, and pair production (20). Neutrons may be in either group depending on the nature of their interaction with matter. This classification is based on the difference in the specific ionization of the light and heavy particles. The specific ionization is from one to three orders of magnitude higher for group two particles than for group one particles. Not only does this mean that the primary ion pairs along the paths are closer for group two, but in addition the delta tracks or spurs along the paths are closer. These spurs are secondary tracks of ionization which are produced by the electrons ejected in the primary ionization process.

For higher specific ionization, as with the heavy particles, the yield of H_2 and H_2O_2 increases indicating the importance of equations (8), (9), and (10). This dependence of H_2 and H_2O_2 yield on specific ionization can be explained as follows. When the specific ionization is high and the local density of free radicals is correspondingly high, the reactions between the free radicals, equations (8), (9), and (10), proceed more rapidly. On the other hand, when the specific ionization is

low and the accompanying delta tracks are far apart, the free radicals diffuse into the main body of the system, reacting with H_2 and H_2O_2 according to equations (11) and (12).

The absorption of x-rays by matter is almost wholly by the photoelectric effect with a slight contribution from the compton effect. In either case the energy absorption is dependent on the atomic number of the system and therefore on the density of electrons. In solutions of low solute concentration it would, therefore, be expected that practically all of the x-ray absorption would occur in the solvent as it contains the majority of the electrons. For this reason, radiation induced oxidation and reduction reactions in dilute aqueous solutions can be followed through the reactions of the free radicals produced by the radiation decomposition of water.

Measurement of Absorbed Dose

In the ferrous-ferric system it was found that the amount of Fe(II) oxidized to Fe(III) was proportional to the total absorbed dose over a wide range of total dose and dose rates. Absorbed dose has units of energy per unit mass and may be represented by dE/dM. dE/dM is related to S_m, the ratio of the mass stopping power of the solution to that of air (a constant for dilute aqueous solutions); W, the absorbed radiation energy required to form an ion pair in air (taken to be 32.5 ev.); and J, the ionization produced per unit mass in air, by the equation

$$dE/dM = S_m WJ. \qquad (22)$$

J is measured for the system under consideration by use of a standard ion chamber irradiated under the same conditions as the sample. The G value of the ferrous-ferric system is determined by use of equation (22) and analytical determination of the number of Fe(II) oxidized when the system is irradiated. For more accurate determination of G, equation (22) should be integrated over the volume of solution under consideration, as S_m is dependent on the energy of the photons, and the photon energy decreases as the photons pass through the solution. The G value of the ferrous-ferric system has been determined as 15.45 ± 0.11 (10). This value is valid for solutions of ferrous sulfate concentration over the range from 10^{-2} to 10^{-5} molar and sulfuric acid concentration from 0.2 to 2.0 normal irradiated with energy from 100 Kev. x-rays to 2 Mev. gamma rays when the total absorbed dose varies from 0 to 50,000 and the dose rate varies from 1/50 to 200 rads/sec. Advantage can be made of this G value in measurement of absorbed energy in other systems for which the G value is to be determined.

EXPERIMENTAL

Preparation of Solutions

All solutions were prepared from Reagent Grade compounds and doubly distilled water. Mo(VI) solutions were prepared by dissolving sodium molybdate in dilute HCl solution. Mo(V)

solutions were prepared by shaking Mo(VI) solutions 3N in HCl in a mercury reductor as suggested by Furman and Murray (8). The normality of the Mo(V) solutions was determined by colorimetric titrations with standard solutions of ceric sulfate using ferroin as indicator and syrupy phosphoric acid as catalyst as suggested by Rao and Suryanarayana (21). This method was used in analyzing Mo(V) solutions before and after irradiation. It was found that good end points could be obtained even with ceric concentrations as low as 0.005N.

The standard solutions of ceric sulfate were prepared by dissolving ceric sulfate in 1N H_2SO_4 and titrating against a standard solution of sodium oxalate prepared from a sample supplied by the U.S. Bureau of Standards. The oxalate solutions were held at 60°C and the endpoints were determined colorimetrically (29).

The ferrous sulfate dosimeter solutions used were approximately 0.005N in ferrous sulfate dissolved in 0.8N H_2SO_4. The ferric solutions for the spectrophotometric calibration curve were standardized by reducing a sample quantitatively to ferrous in a Jones Reductor (26) and titrating with a standard solution of $KMnO_4$. The $KMnO_4$ solution was standardized against a standard solution of sodium oxalate.

The acidity of the solutions was measured by titration against a standard solution of sodium carbonate (26).

Spectrophotometric Analyses

A Beckman model D.U. spectrophotometer was used in all absorbance ($\log_{10} I_0/I$, where I_0 is the light intensity incident on a sample and I is the light intensity transmitted by a sample) measurements. The cells used were matched Beckman Corex cells of 1 cm. x 1 cm. x 4.8 cm.

A calibration curve for the spectrophotometric analysis of Fe(III), Fig. 2, was obtained by quantitative dilution of samples of standard Fe(III) solution.

The analysis of the irradiated solutions required that Mo(V) or Mo(VI) be determined in the presence of the other. No method of analysis of this type was found in the literature. The method of spectrophotometric analysis for Mo(VI) based on the reduction of Mo(VI) to Mo(V) with stannous chloride and measurement of absorbance of the Mo(V) thiocyanate complex (12) was tried without the addition of stannous chloride in hopes that Mo(V) could be determined in a mixture of both. This method was found unreliable.

The only reproducible method found was analysis of Mo(V) in HCl solutions making use of the natural Mo(V) absorbance (12). 400mμ was found to be a suitable wavelength as the absorbance of Mo(VI) was negligible at this wavelength. The calibration curve obtained for Mo(V) solutions is shown in Fig. 1.

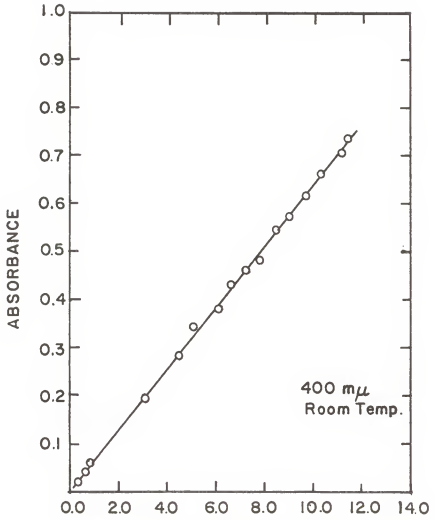

Fig 1 Mo (V) calibration curve.

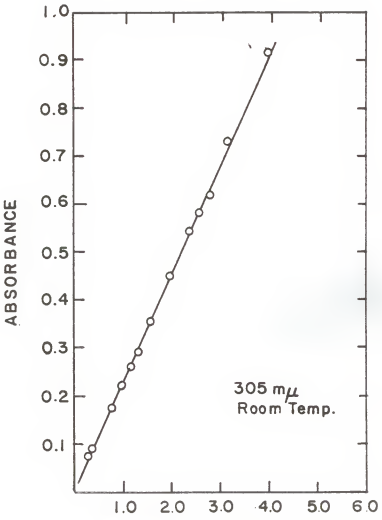

Fig. 2 Ferric calibration curve

Temperature Dependence of Mo(V) Absorbance

Solutions of known Mo(V) concentration in various HCl acid media were heated to approximately 80°C and poured into an absorption cell. The cell was then placed in the spectrophotometer. Using a small bulb mercury thermometer, the cooling curve, Fig. 3, of the solution was obtained. Another amount of the same solution was heated to about 80°C and poured into the same absorption cell. The cell was placed in the spectrophotometer and the same thermometer was inserted in the cell. As soon as the sample cooled to 60°C, a stopclock was started, the thermometer removed, and the cell compartment cover was put in place. Absorbance data at a fixed wavelength were then collected and the exact corresponding cooling time was recorded. A typical curve obtained in this manner is shown in Fig. 4. The same procedure was repeated at several wavelengths from 350mμ to 450mμ. This range was selected on the basis that it included the absorption peaks corresponding to the HCl acid normalities of the Mo(V) solution investigated (13). From the cooling curves and the time vs. absorbance curves the corresponding absorbance vs. temperature curves were obtained.

X-ray Irradiations

The Kansas State University Nuclear Engineering Department X-ray machine, shown in Fig. 5, was used in all sample irradiations. The X-ray machine is a 150 K.V. Westinghouse

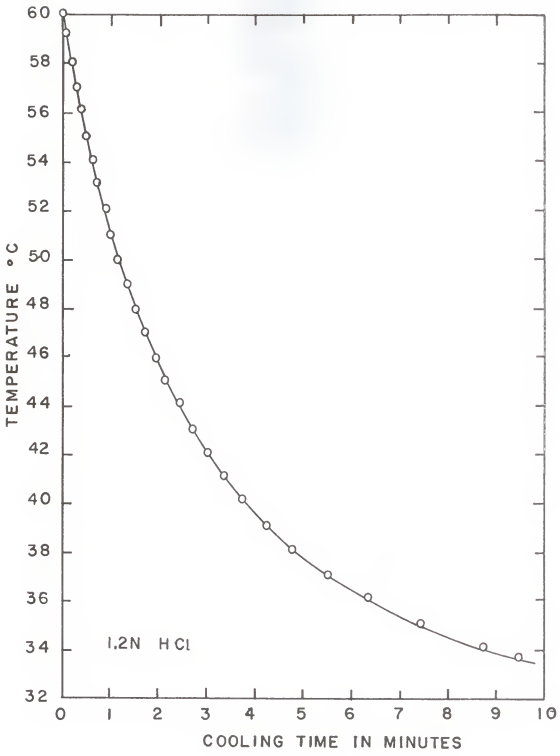

Fig. 3 Typical cooling curve for Mo (V) solution

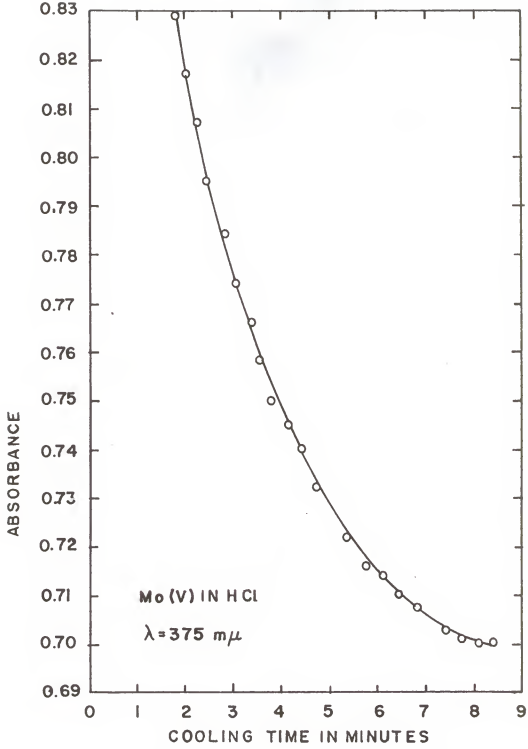

Fig. 4 Typical absorbance vs. cooling time curve for Mo (V) solution in HCl

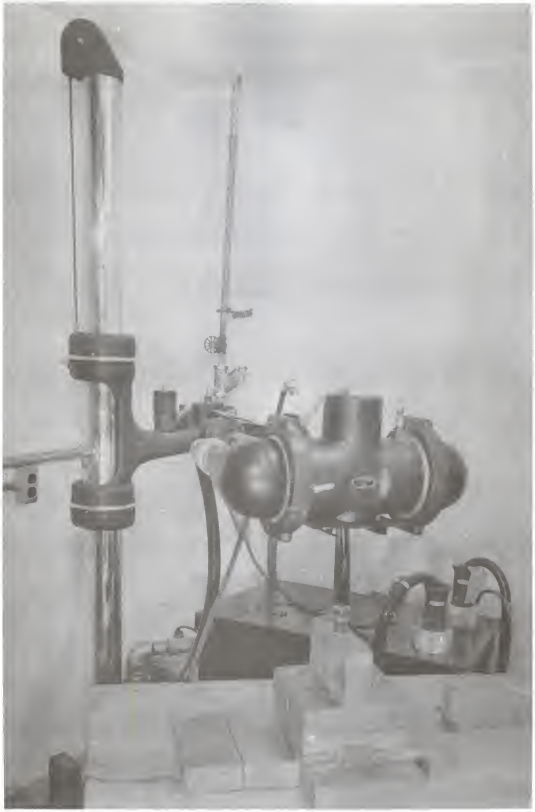

Fig. 5 Photograph of the X-ray unit and cells used.

Thermax industrial unit. The kilovoltage can be regulated from 50 to 150 in 2 K.V. intervals and the milliamperage can be adjusted from 4 to 15 ma. The X-ray tube has a tungsten target and, therefore, gives a beam with a continuous spectrum. The tube is cooled by circulating water. A built-in stabilizer is included in the X-ray machine control panel to stabilize the X-ray dose during small changes of the line voltage. The control panel has a time set that can be used in adjusting the sample exposure time in one second intervals from 0 to 60 min. The X-ray machine was enclosed in a room with a lead lined door which was kept closed during irradiation.

A series of ferrous sulfate solutions were irradiated for various time intervals ranging from 2 to 20 minutes in 2 minute steps to investigate the constancy of the absorbed dose. The amount of ferrous oxidized to the ferric state was determined spectrophotometrically at 305mμ. Figure 6 shows that the ferric absorbance increase is linear with exposure time indicating that the X-ray beam intensity is constant with time. Solutions of varying Mo(V) concentration in HCl and H_2SO_4 media were irradiated for a constant time to investigate the dependence of the irradiation effect on Mo(V) concentration. Other solutions of constant Mo(V) concentration were irradiated for different time intervals from 30 to 210 minutes to investigate the effect of absorbed dose. The Mo(V) concentrations before and after irradiation were analyzed either spectrophotometrically at 400mμ or by

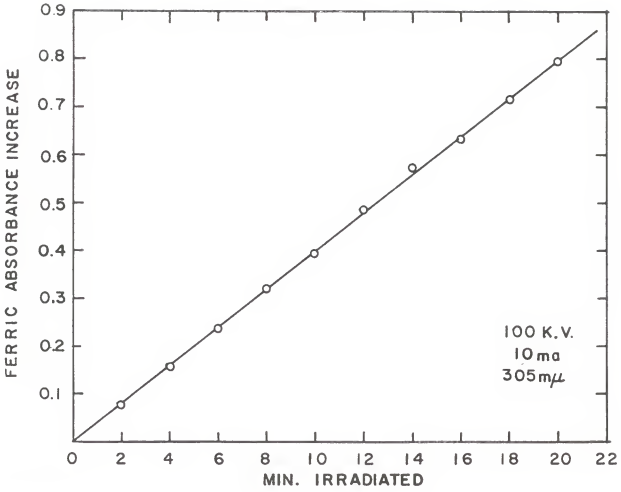

Fig 6. Plot showing linearity of absorbance increase with irradiation time.

titration with ceric sulfate. The irradiation vessels used were commercial ground glass covered EXAX 29/12 bottles of approximately 15cc total volume. These vessels were pre-irradiated as suggested by Rigg, Stein, and Weiss (22). This pre-irradiation served the purpose of saturating the glass with X-rays of preferred absorption.

Each irradiation of a Mo(V) sample was followed by an irradiation of the ferrous sulfate dosimeter solution under the same conditions to determine the total absorbed dose.

Several solutions of Mo(V) were evacuated before irradiation to make it possible to compare the G value in the presence and absence of dissolved oxygen. The Mo(V) concentration change during irradiation was determined either spectrophotometrically or by titration, using as a blank an aliquot of that Mo(V) solution evacuated under the same conditions. A schematic diagram of one of the vessels used in the irradiations under vacuum is shown in Fig. 7. The tapered end was sealed by fusion after filling with solution and the ground glass end was connected to the vacuum system. After irradiation the tapered end was broken and the solution was drained out.

Stability of Mo(V) Solutions

Solutions of Mo(V) in 2N HCl were heated and held at temperatures of 30, 40, 50, and 60°C in a constant temperature bath for 3 day periods. At various times during the three

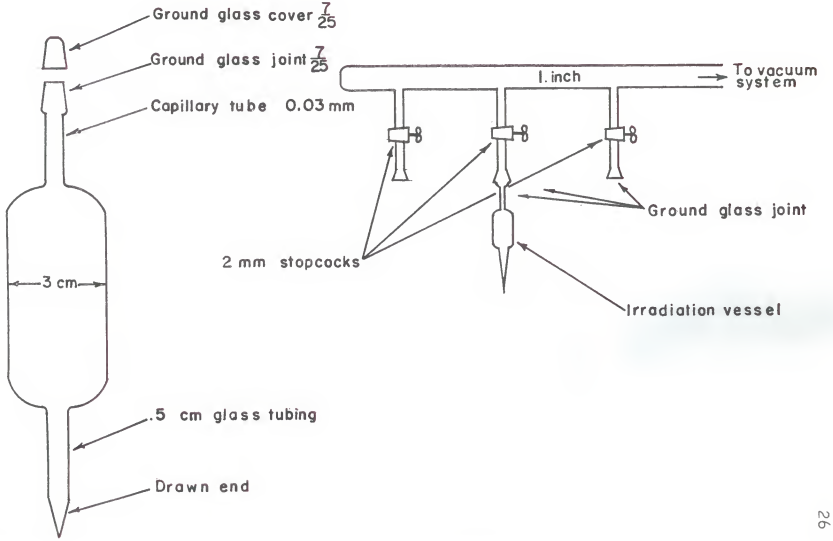

Fig 7. Schematic of irradiation cell and vacuum system attachments.

day periods, aliquots were withdrawn from these constant temperature solutions and analyzed for Mo(V) concentration spectrophotometrically or by titration with ceric sulfate.

Variation of X-ray Beam Intensity with X-ray Machine Kilovoltage and Milliamperage

A scintillation probe was used to measure the count rate of the X-ray beam at various kilovoltage and milliamperage settings. The count rate as seen in Fig. 8 was found to increase rapidly with both the milliamperage and kilovoltage of the X-ray tube. As the milliamperage affects only the intensity of the X-ray spectrum (2), the count rate vs. milliamperage curves at constant kilovoltage are an indication of the variation of photon energy flux with milliamperage. The absorbed dose of irradiated samples would follow this same relation with milliamperage since the absorption probability is constant. This is not the case when the kilovoltage is varied as the kilovoltage affects the shape of the X-ray spectrum.

RESULTS AND DISCUSSION

Temperature Dependence of Mo(V) Spectrophotometry

As will be discussed in more detail later, there is an oxidation of Mo(V) to Mo(VI) on irradiation. Determination of the reaction yields required accurate analysis of Mo(V) solutions before and after irradiation. During irradiation

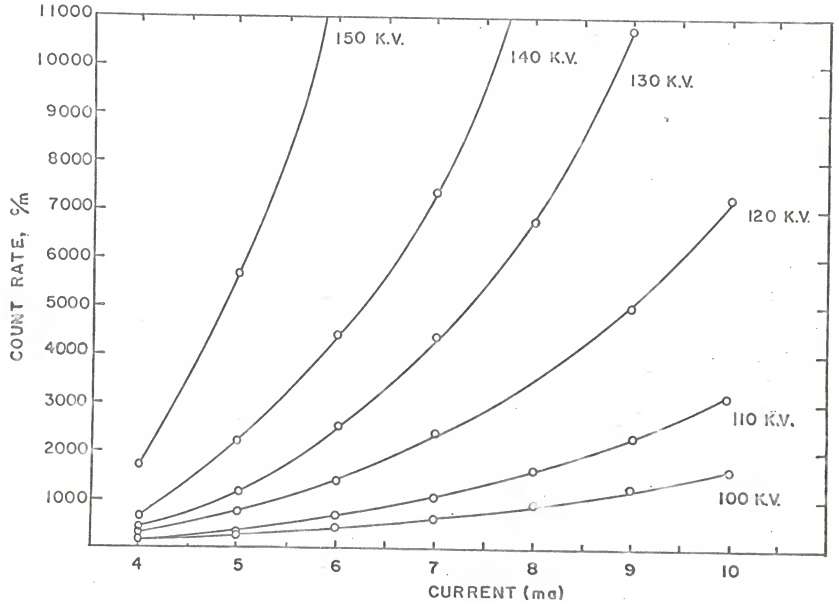

Fig. 8 Variation of count rate with X-ray tube voltage and current.

a heating of the samples was observed. As the irradiated solutions were to be analyzed spectrophotometrically, it was necessary to test the effect of temperature on the light absorbance of the Mo(V) solutions. Preliminary results showed that in some cases a 50 per cent increase in the light absorbance took place by raising the temperature of the solution 20°C.

To the author's knowledge no systematic work has been reported on the temperature effect on light absorbance of Mo(V).

Hiskey and Meloche (13) studied the color phenomena associated with Mo(V) in HCl solutions at room temperature and found that the light absorbance was dependent on the acidity of the solution as well as the wavelength of the light used. A study of the temperature effect necessitated, therefore, investigation of these two parameters. It was also desirable to investigate the applicability of Beer's law at these higher temperatures. The temperature range of interest was from room temperature to 55°C.

From the cooling curves and the time vs. absorbance curves, typical samples of which are shown in Fig. 3 and Fig. 4 respectively, the corresponding absorbance vs. temperature curves were obtained. Tables 1 through 5 show the absorbance vs. temperature data at various wavelengths and various HCl normalities. The plots of these data were linear and an IBM 650 computer program was used to determine the least squares

Table 1. Temperature vs. absorbance data for Mo(V) in 1.2N HCl.

Temperature	Absorbance of various wavelengths				
°C	350mμ	375mμ	400mμ	425mμ	450mμ
52		0.4510	0.4110	0.2920	
50	1.040	0.4990	0.4080	0.2905	
48	1.034	0.4470	0.4060	0.2892	0.1926
46	1.028	0.445	0.4037	0.2878	0.1917
44	1.020	0.4425	0.4011	0.2864	0.1906
42	1.011	0.4402	0.3991	0.2848	0.1895
40	1.002	0.4390	0.3974	0.2834	0.1884
38	0.993	0.4375		0.2820	0.1873
36		0.4365		0.2804	0.1864

Table 2. Temperature vs. absorbance data for Mo(V) in 2N HCl.

Temperature	Absorbance at various wavelengths				
°C	350mμ	375mμ	400mμ	425mμ	450mμ
52				0.366	0.284
50	1.155	0.475	0.451	0.364	0.282
48	1.128	0.4705	0.449	0.362	0.280
46	1.098	0.466	0.446	0.359	0.278
44	1.072	0.461	0.443	0.356	0.275
42	1.045	0.457	0.4405	0.353	0.273
40	1.019	0.453	0.437	0.350	0.271
38	0.995	0.450	0.435	0.348	0.268
36	0.977	0.447	0.433	0.347	
34	0.960		0.4305		

Table 3. Temperature vs. absorbance data for Mo(V) in 3.0N HCl.

Temperature	Absorbance at various wavelengths				
°C	350mμ	375mμ	400mμ	425mμ	450mμ
52				0.596	
50	1.475	0.4535	0.5345	0.568	0.599
48	1.405	0.4425	0.5275	0.5540	0.5770
46	1.350	0.4340	0.5205	0.5360	0.5550
44	1.305	0.4270	0.5135	0.5220	0.5350
42	1.270	0.4210	0.5075	0.5080	0.5180
40		0.4165	0.5025	0.4975	0.5020
38		0.4125	0.4980	0.4860	
36				0.477	

Table 4. Temperature vs. absorbance data for Mo(V) in 3.6N HCl.

Temperature	Absorbance at various wavelengths				
°C	360mμ	375mμ	400mμ	425mμ	450mμ
52	1.505			0.608	
50	1.450	0.675		0.590	0.657
48	1.40	0.660	0.527	0.576	0.636
46	1.35	0.644	0.520	0.562	0.615
44	1.300	0.630	0.513	0.545	0.594
42	1.240	0.616	0.506	0.535	0.576
40	1.190	0.604	0.500	0.523	0.557
38	1.140	0.593	0.495	0.513	0.540
36	1.110	0.582	0.492	0.506	0.523
34		0.572		0.503	0.514

Table 5. Temperature vs. absorbance data for Mo(V) in 4.0N HCl.

Temperature	Absorbance at various wavelengths				
°C	350mμ	375mμ	400mμ	425mμ	450mμ
50	2.52		0.792	0.975	1.05
48	2.46		0.781	0.955	1.01
46	2.36	0.813	0.771	0.935	0.972
44	2.275	0.789	0.760	0.912	0.925
42	2.19	0.766	0.747	0.887	0.890
40	2.12	0.743	0.735	0.864	0.855
38	2.04	0.721	0.723	0.840	0.824
36	1.98	0.702	0.713	0.820	0.795

slopes and intercepts. The least square slopes are tabulated in Table 6 as a function of acidity and wavelength.

A. Beer's Law. Hiskey and Meloche (13) found that Beer's law was obeyed at room temperature for solutions 0.01N in Mo(V). From the plots of absorbance, A, vs. temperature, T, at different Mo(V) concentrations, C, data were extracted of absorbance vs. Mo(V) concentration at constant temperature. The resulting plots were linear indicating that Beer's law holds up to ^{o}50 C. This relation can be represented mathematically by

$$(\partial A/\partial C)_T = A_0. \tag{23}$$

It can therefore be assumed that no alteration of the Mo(V) molecules takes place in this temperature range. Figure 9 shows a plot of this data at 30^{o}C and 50^{o}C for Mo(V) solutions in 2N HCl. The absorbance was measured at 400mμ. The least squares slopes of these lines were obtained at 5^{o}C intervals from 30^{o}C to 50^{o}C and are tabluated in Table 7. The slopes are plotted against temperature in Fig. 10. The linearity of the curve suggests the equation

$$dA/dC = a_1 + a_2T, \tag{24}$$

and shows that the molar extinction coefficient is a linear function of temperature.

B. The Effect of Temperature on Variation of Absorbance with Wavelength, λ, at Constant Acidity, N, and Mo(V) Concentration, C. Figure 11 shows that the temperature does not affect the shape of the A vs. λ curve. It, therefore, does not affect the position of the absorption peaks.

Table 6. Slope of temperature dependence of absorbance lines for solutions of 6.70×10^{-3}N Mo(V) in varying acid concentration at various wavelengths.

λ	Slope (absorbance units/°C). Temperature range 30°C to 55°C				
mμ	1.2N HCl	2.0N HCl	3.0N HCl	3.6N HCl	4.0N HCl
350	0.003964	0.01243	0.0255		0.3979
360				0.02533	
375	0.000940	0.002074	0.003357	0.00645	0.01117
400	0.001114	0.001316	0.003080	0.003689	0.005738
425	0.000704	0.001283	0.007175	0.004664	0.01129
450	0.000528	0.001136	0.009742	0.009233	0.01845

Table 7. Slope of absorbance vs. concentration lines at different temperatures for Mo(V) solutions in 2N HCl. The absorbance was measured at 400mμ.

Temperature	Slope
°C	Absorbance units/ unit molarity Mo(V)
30	61.27
35	62.58
40	63.70
45	64.86
50	66.10

Table 8. Slope of absorbance vs. temperature lines for various Mo(V) concentrations in 2N HCl. The absorbance was measured at 400mμ.

10^3 x Mo(V) normality	10^3 x slope
moles/liter	Absorbance units/°C
1.5	0.355
2.0	0.406
3.5	0.600
6.6	1.265
7.3	1.870
10.6	2.440

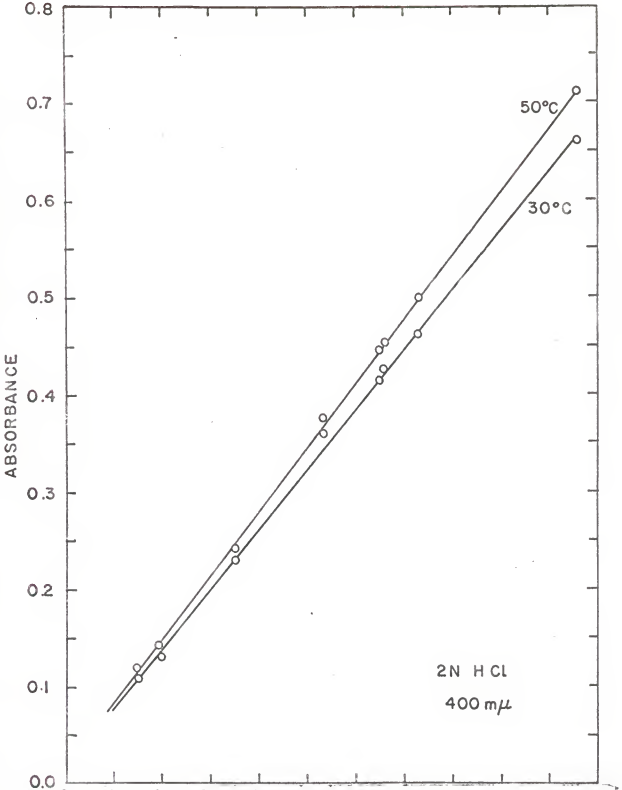

Fig. 9 Absorbance vs. Mo(V) Concentration at 30 C and 50 C.

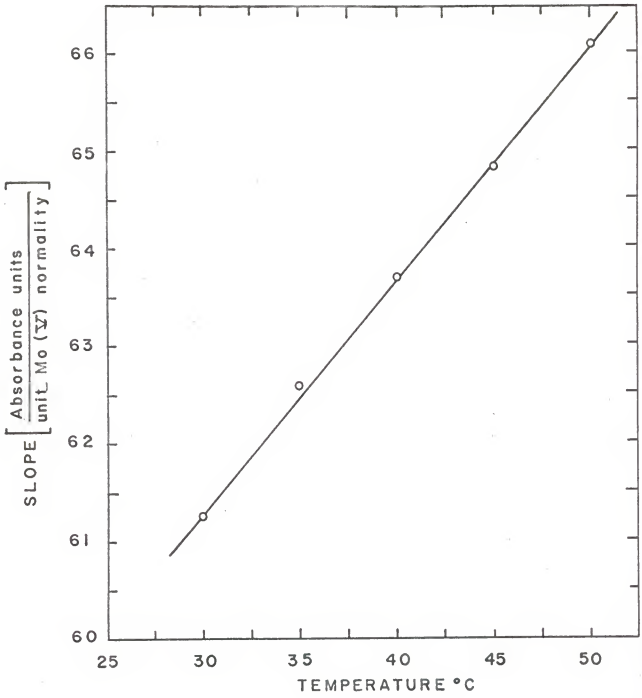

Fig. 10 Effect of temperature on slope of absorbance vs Mo (VI) concentration lines.

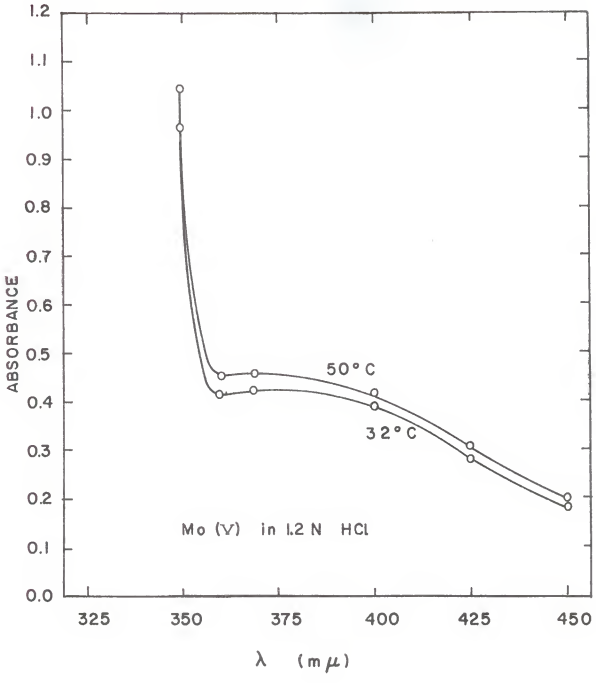

Fig. 11 Effect of temperature on variation of absorbance with wave length.

C. The Effect of Temperature on Variation of Absorbance with the HCl Normality of the Mo(V) Solutions at Constant Wavelength and Mo(V) Concentration. The absorbance vs. acidity curves obtained at all temperatures in this investigation are in agreement with the general shape of those reported by Hiskey and Meloche (13) at room temperature. That is, the absorbance increases with the increase in normality. The rate of change of absorbance with acidity, however, depends on the wavelength used. Figure 12 illustrates the effect of temperature on the A vs. N plot.

D. The Effect of Wavelength, λ, on Variation of Absorbance with Temperature at Constant Acidity and Mo(V) Concentration. At a specific wavelength, the absorbance of a solution increases linearly with temperature, that is to say,

$$(\partial A/\partial T)_C = a_3. \qquad (25)$$

A group of such straight lines obtained at different wavelengths is shown in Fig. 13. The slopes, dA/dT, of these lines are plotted vs. λ in Fig. 14. It is obvious that the effect of wavelength on dA/dT depends on the acidity of the solution. Each of these curves has a minimum. The minimum shifts toward a lower wavelength as the acidity increases. It is further observed that 400mμ is, in almost all cases, close to the minimum. This qualifies 400mμ as an optimum wavelength to use in Mo(V) analysis from the point of view of the temperature effect in this range of acidity and wavelength.

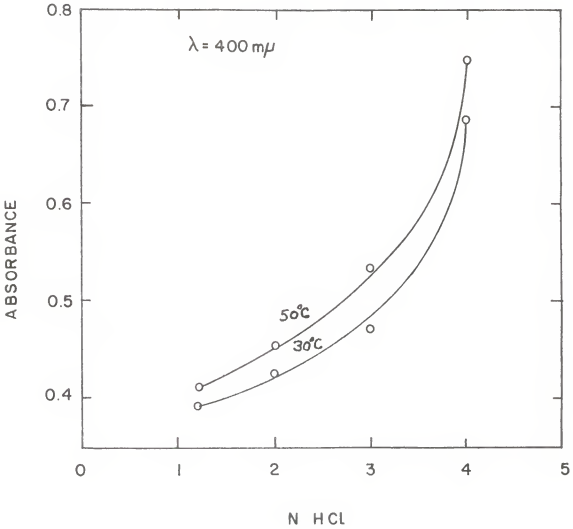

Fig 12. Effect of temperature on absorbance in different acid normalities.

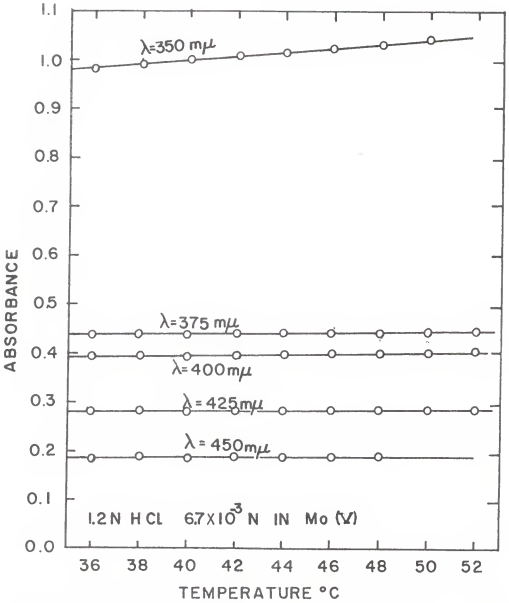

Fig. 13 Absorbance vs. temperature at various wavelengths.

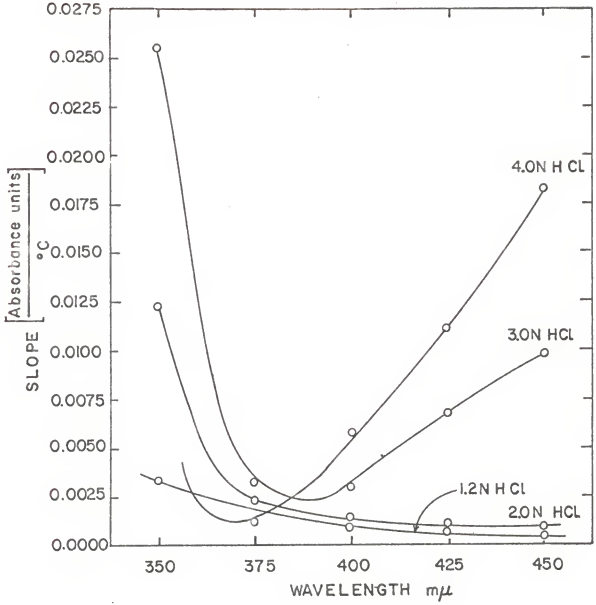

Fig 14 Slope of absorbance vs. temperature plots at various wavelengths and acidities.

E. The Effect of Acidity on Variation of Absorbance with Wavelength. Figure 15 is a typical sample of the groups of curves obtained at different temperatures. The acidity is seen to increase the absorbance in general and to shift the minima to higher wavelengths. Comparison of Fig. 15 with similar curves (not included) showed that the temperature does not affect the general shape of the curves in relation to one another.

F. The Effect of Acidity and Wavelength on the Temperature Dependence of Absorbance, dA/dT. The acidity increases the temperature dependence in general, as can be seen by Fig. 16. The temperature dependence passes through a minimum near 400mμ as the wavelength is increased from 350mμ to 450mμ.

G. The Effect of Mo(V) Concentration on the Temperature Dependence of Absorbance, dA/dT. Figure 17 shows a plot of the temperature dependence of absorbance vs. Mo(V) concentration. The relation can be represented by,

$$dA/dT = a_4 + a_5C. \qquad (26)$$

The slopes and concentrations used in plotting this line are listed in Table 8.

H. Development of an Equation Representing Absorbance as a Function of Temperature and Mo(V) Concentration. As shown in part A,

$$(\partial A/\partial C)_T = a_0$$

and

$$dA/dC = a_1 + a_2T.$$

Also, from part D,

$$(\partial A/\partial T)_C = a_3$$

and from part G,

$$dA/dT = a_4 + a_5C.$$

C and T being independent variables, the solution of this set of differential equations can be written in the form

$$A = K_0 + K_1C + K_2T + K_3CT \text{ (Appendix B).} \qquad (27)$$

The four constants in this equation can be determined by selecting a set of four experimental absorbance values determined at different, widely spread temperatures and concentrations, and solving the resulting four simultaneous equations. Three such sets were solved and the resulting constants are shown in Table 9. Experimental and computed absorbances for a set of arbitrarily chosen points have been included in Table 10 for comparison. One set of four good experimental points may yield satisfactory constants. However, it is advisable to take two or more sets and average the absorbances calculated. The average values obtained as such are shown in column 6 of Table 10.

An alternative method of determining constants, K_i, would be to apply the least squares method of analysis (30) to the matrix resulting from n experimental data points where n is greater than 4 (Appendix C). An IBM 650 program has been prepared that reduces the n by 4 matrix equations to a set of 4 simultaneous equations and solves them by a Crout reduction. A set of 20 experimental points has been chosen and values of

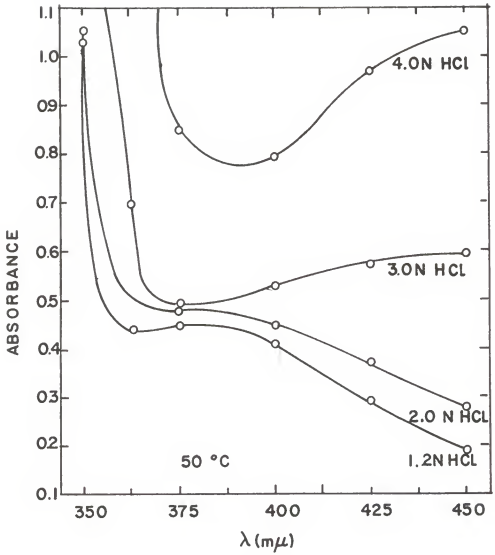

Fig. 15 Absorbance vs wavelengths at various acidities at 50 ° C.

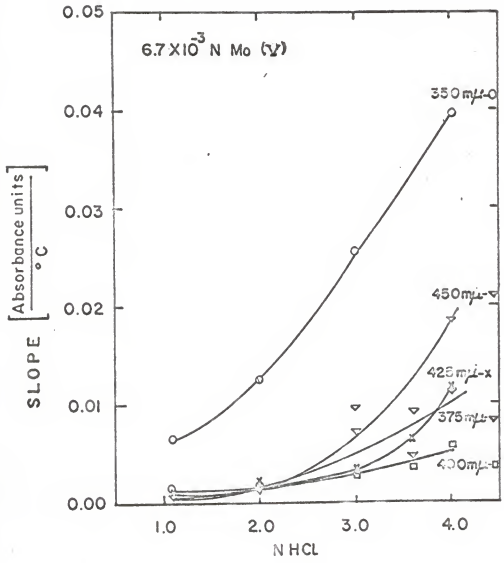

Fig. 16 Temperature dependence of absorbance at various wavelengths and acidities.

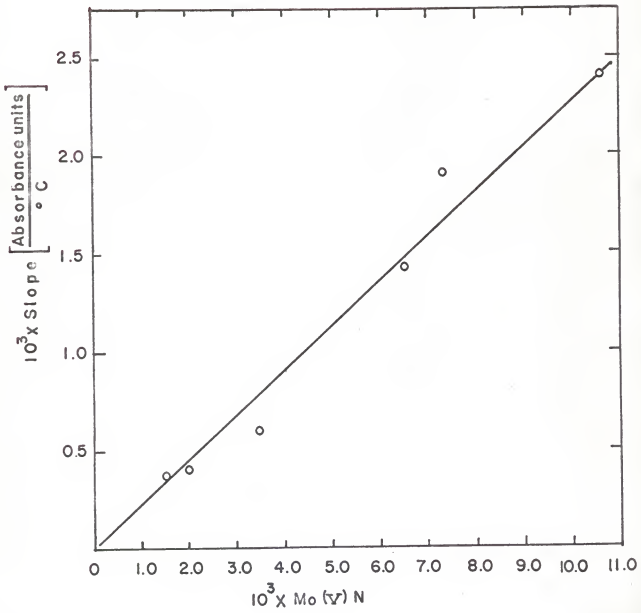

Fig. 17. Effect of Mo(V) concentration on temperature dependence of absorbance.

Table 9. Constants determined by simultaneous equations method and least squares method.

Method	Constants			
	K_0	K_1	K_2	K_3
Simultaneous equations				
Group 1	7.93×10^{-2}	5.58×10^{1}	-1.60×10^{-3}	2.33×10^{-1}
Group 2	-9.53×10^{-3}	7.78×10^{1}	5.88×10^{-4}	-2.99×10^{-1}
Group 3	-4.77×10^{-3}	7.49×10^{1}	4.98×10^{-4}	-2.60×10^{-1}
Least squares	2.83×10^{-2}	5.46×10^{1}	-3.09×10^{-4}	2.32×10^{-1}

the constants, K_1, have been determined by this least squares method. The absorbance values computed using this set of constants are shown in column 7 of Table 10.

Based on a sufficiently large number of points to give good statistics, it can be said that the results obtained by the least squares method of analysis are in better agreement with the experimental values than those obtained by the simultaneous equations method. The maximum deviation was ± 4 per cent as compared to ± 7 per cent. However, the mean percentage error,

$$1/m \sum_{i=1}^{m} (A_{i\text{-obs}} - A_{i\text{-calcd}}) 100/A_{i\text{-obs}}, \qquad (28)$$

where m denotes the number of points considered, was calculated for both A (average) and A (least squares). Both were found to be close to 1 per cent.

It can be concluded that in general the temperature must be considered in computing Mo(V) concentrations from absorbance measurements. An experimenter can, by taking a limited number of observations, calculate the constants of the absorbance equation. He can then use the equation to calculate the concentration of Mo(V) in any solution of known absorbance and temperature within the range investigated.

Stability of Mo(V)

Solutions of Mo(V) are known to be unstable, undergoing an oxidation reaction to Mo(VI) on standing in an air atmosphere

Table 10. Comparison of calculated to observed absorbances.

C	T	A, simultaneous equations				A	A
Mo(V) normality	C	Group 1	Group 2	Group 3	average	Least Squares	Observed
6.7×10^{-3}	50.0	0.451	0.454	0.440	0.444	0.455	0.451
3.5×10^{-3}	50.0	0.242	0.240	0.235	0.239	0.244	0.240
6.6×10^{-3}	32.3	0.421	0.440	0.450	0.439	0.428	0.428
1.5×10^{-3}	36.0	0.116	0.112	0.105	0.111	0.111	0.112
5.4×10^{-3}	33.7	0.366	0.377	0.364	0.369	0.352	0.366

at room temperature. As the temperature of the irradiated Mo(V) samples has been observed to increase to about 35°C, it was desirable to investigate the effect of temperature on the autoxidation of Mo(V) to Mo(VI). Solutions of Mo(V) in 2N HCl were held at temperatures of 30, 40, 50, and 60°C for three day periods. The solutions were analyzed at various times during this period. It was found that the oxidation is enhanced by increasing the temperature. Table 11 shows the concentration of the solutions as a function of time. This data is plotted in Fig. 18. The curves appeared to be nearly linear for the initial 35 hours. The slopes of the linear parts from 0 to 35 hours are tabulated in Table 12 along with the reciprocal of the corresponding temperature.

Table 12. Slope of Mo(V) stability curves at different temperatures.

10^3 x Slope	Temperature	10^3 x $1/T°K$
moles/liter-hr.	°C	$°K^{-1}$
1.36	30	3.300
1.89	40	3.195
2.84	50	3.096
3.98	60	3.003

These data are plotted in Fig. 19 which can be used to interpolate for the slope of the stability curve at different temperatures.

For an initial Mo(V) concentration of 9.0 x 10^{-3} moles/liter

Table 11. Data for stability study of Mo(V) at various temperatures.

Temperature												
30 °C			40 °C			50 °C			60 °C			
Time		Concentration	Time		Concentration	Time		Concentration	Time		Concentration	
hr	min	moles/liter	hr	min	moles/liter	hr	min	moles/liter	hr	min	moles/liter	
0	0	9.63×10^{-3}	0	0	8.98×10^{-3}	0	0	8.46×10^{-3}	0	0	8.30×10^{-3}	
0	35	9.55	1	0	8.84	1	30	8.40	2	25	8.18	
2	0	9.48	2	0	8.83	3	50	8.39	4	25	8.10	
4	30	9.41	3	0	8.77	7	50	8.26	6	25	8.08	
6	30	9.39	4	0	8.77	18	5	7.96	9	10	8.03	
9	5	9.34	8	50	8.73	19	10	7.92	20	0	7.65	
17	5	9.25	19	5	8.50	20	30	7.88	22	25	7.55	
18	45	9.22	21	0	8.43	22	50	7.82	25	50	7.38	
21	45	9.20	23	50	8.42	24	20	7.82	28	25	7.25	
23	25	9.18	25	50	8.36	26	55	7.75	35	40	6.95	
25	10	9.12	26	55	8.35	42	5	7.13	44	35	6.49	
29	35	9.06	29	5	8.25	44	20	7.05	46	10	6.27	
32	0	9.05	42	35	8.05	46	35	6.95	49	25	6.05	
40	0	8.96	43	40	8.04	48	5	6.92	51	55	5.70	
42	35	8.88	46	5	7.98	49	25	6.79	56	20	5.33	
44	0	8.88	49	45	7.90	66	30	6.18	69	10	4.21	
45	40	8.85	53	40	7.80	71	35	5.97	71	30	3.98	

Table 11. (concl.)

Temperature								
30°C			40°C			50°C			60°C		
Time		Concentration	Time		Concentration	Time		Concentration	Time		Concentration
hr	min	moles/liter	hr	min	moles/liter	hr	min	moles/liter	hr	min	moles/liter
48	5	8.79×10^{-3}	58	20	7.68×10^{-3}	74	25	5.90×10^{-3}	72	50	3.89×10^{-3}
51	0	8.79	69	45	7.40				73	50	3.84
53	50	8.76	72	0	7.30				75	30	3.70
65	15	8.50							76	30	3.59
69	20	8.35							80	10	3.33

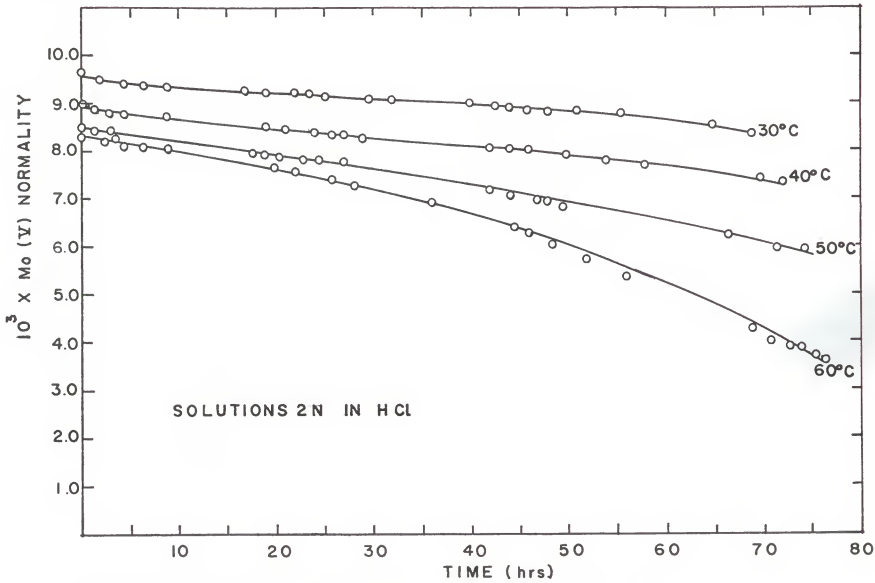

Fig. 18 Oxidation of Mo(V) to Mo(VI) at various temperatures.

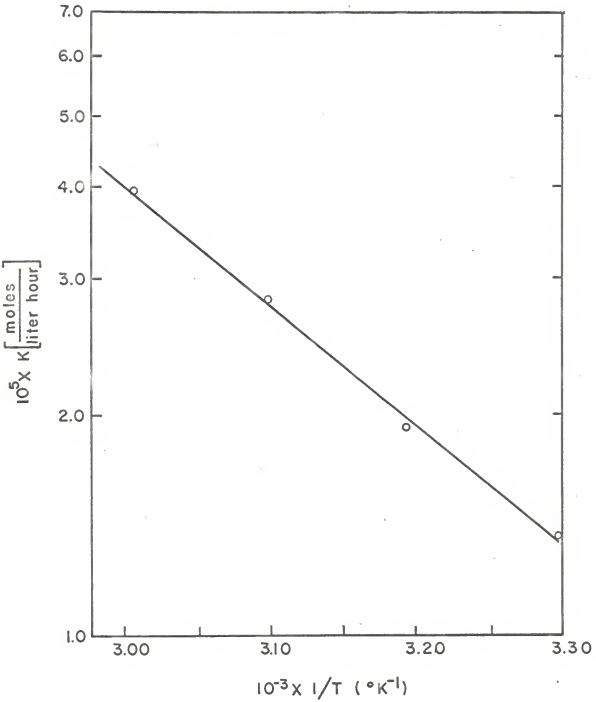

Fig. 19 Plot of Mo(V) stability constant vs. reciprocal temperature.

(a typical concentration in the irradiation study), the room temperature (28.5°C) autoxidation rate constant has been interpolated as 1.25×10^{-5} moles/liter-hour. The rate constant for a sample heated to 35.5 C was 2.40×10^{-3} moles/liter-hour. The concentration decrease per hour due to the difference in the autoxidation rates would be 1.5×10^{-6} moles Mo(V)/liter. This concentration decrease was well within the experimental error of the Mo(VI) irradiation yield determinations. For this reason no corrections for the autoxidation of Mo(V) to Mo(VI) had to be subtracted from the irradiation induced oxidation of Mo(V) to Mo(VI). For longer irradiation times and/or higher irradiation intensities, which would cause the temperature rise to increase, this autoxidation could become considerable.

X-ray Irradiations

A. Effect of X-rays on Molybdenum Ions. Irradiated samples of Mo(V) were observed to require less oxidizing agent to neutralize after irradiation with X-rays than before irradiation. As mentioned in the experimental section, ceric sulfate was the oxidizing agent used. Table 13 shows a typical set of data.

Table 13. Mo(V) inventory by titration during an irradiation

Initial Mo(V) concentration	ceric before	ceric after	Time irradiated	Calculated G value
moles/liter	ml.	ml.	min.	ions oxidized/100ev.
3.06×10^{-3}	2.30 ± 0.05	1.39 ± 0.05	60	7.67 ± 0.84

The change in the Mo(V) concentration on irradiation was determined both by volumetric and spectrophotometric analyses. The G value of the Mo(V) to Mo(VI) system was calculated from titration data making use of the ferrous dosimeter (discussed in detail in the experimental section) and the following equation:

$$G_{(Mo)} = G_{(Fe)} \times T_{Fe}/T_{Mo} \times Y_{Mo(VI)}/Y_{Fe(III)}. \quad (29)$$

T_{Fe} = exposure time of ferrous sulfate solution (min).

T_{Mo} = exposure time of Mo(V) solution (min).

$Y_{Mo(VI)}$ = yield of Mo(VI) as calculated from titrimetric analysis before and after irradiation (moles/liter-min).

$Y_{Fe(III)}$ = yield of Fe(III) as calculated from absorbance at λ = 305mμ and the calibration curve, Fig. 4 (moles/liter-min).

G_{Fe} = G value of Fe(II) to Fe(III) system (15.45 ± 0.11 ions oxidized/100ev, as mentioned in theory).

Each irradiation of a Mo(V) sample was followed by an irradiation of a ferrous dosimeter sample at the same x-ray

machine kilovoltage and milliamperage and the same geometry.

The G value of the Mo(V) to Mo(VI) system was calculated from light absorbance data using the same equation and the calibration curve for Mo(V) analysis (shown in the experimental section) to determine the Mo(VI) yield. Table 14 shows a typical set of absorbance data for an irradiated Mo(V) sample.

Table 14. Mo(V) inventory by absorbance during an irradiation.

Initial Mo(V) concentration	Absorbance decrease	Time irradiated	Calculated G value
moles/liter	absorbance units	min	ions oxidized/100ev.
3.06×10^{-3}	0.077±0.010	120	8.98±1.30

As is shown in Table 13, less ceric is required for the irradiated solutions. This indicates that fewer milli-equivalents of oxidizable ions such as Mo(III), Mo(IV), and Mo(V) were present after irradiation than before. That the absorbance of the irradiated samples was less than the absorbance of the unirradiated samples indicated that the Mo(V) concentration was reduced. Table 15 shows a comparison of typical results obtained from both absorbance and titration data.

Table 15. Comparison of concentration change of Mo(V) determined spectrophotometrically and Mo(VI) yields determined titrimetrically for one hour irradiations.

10^3 x Mo(V) concentration by absorbance	10^3 x Mo(VI) yield by titration
moles/liter	moles/liter
1.30±0.18	1.34±0.14
1.16±0.21	1.26±0.15
1.40±0.16	1.41±0.15
1.27±0.15	1.21±0.16
1.38±0.15	1.49±0.16

The first column of the table shows the absolute decrease in the Mo(V) concentration as determined by reference to the Mo(V) standardization curve Fig. 3. The second column shows the Mo(VI) yield based on the assumption that the change in the Mo(V) concentration was due only to the oxidation of Mo(V) to Mo(VI). The quantitative agreement in the Mo(V) concentration decrease and the Mo(VI) yield makes it possible to express the overall effect of X-rays on Mo(V) samples as the oxidation of Mo(V) to Mo(VI),

$$\text{Mo(V)} \xrightarrow{\text{X-rays}} \text{Mo(VI)}, \qquad (30)$$

rather than a combination of oxidation to Mo(VI) and reduction to Mo(III) and Mo(IV).

As the Mo(V) solutions were very dilute it could be safely assumed that the observed oxidation occurred through

the diffusion and reaction of the radiation decomposition products of water with Mo(V).

Samples of Mo(VI) were irradiated and analyzed spectrophotometrically and by titration. No change in the ceric requirement or the light absorbance was observed in the irradiated samples. This indicates that the rate of the reaction between Mo(VI) and the reducing radiation decomposition products of water is less than the rate of reaction of Mo(V) with the oxidizing products.

B. Effect of Absorbed Dose on Mo(VI) Yields. Mo(V) samples were irradiated for various lengths of time at a constant dose rate. The G values of the Mo(V) to Mo(VI) reaction were calculated from the Mo(VI) yields and are tabulated in Table 16. The least squares line fitting these results is

$$G = 9.43 - 4.75 \times 10^{-3}t, \tag{31}$$

where t is exposure time in minutes. This line is superimposed on the data in Fig. 20. The 95 per cent confidence limits of the slope were calculated (19) using the equation

$$95\% \text{ variance} = \pm 1.96 \left[\frac{\sum_{i=1}^{n} y_i^2 - a \sum_{i=1}^{n} y_i - b \sum_{i=1}^{n} x_i y_i}{(n-2)\left\{ \sum_{i=1}^{n} x_i^2 - \left(\sum_{i=1}^{n} x_i \right)^2 / n \right\}} \right]. \tag{32}$$

This equation shows that there is a 95 per cent probability that the slope = -0.0047 ± 0.0162.

In the ferrous-ferric system the irradiation yield, y, has been observed to be proportional to absorbed dose, D, up to approximately 50,000 rads. That is, $y = K_1 D$ where K is a

Table 16. G values as a function of irradiation time.

Sample number	Irradiation time	G
	min	ions oxidized/100ev.
1	40	10.3
2	40	8.8
3	60	10.2
4	60	9.05
5	60	9.15
6	90	9.8
7	90	8.6
8	90	8.3
9	120	8.8
10	120	8.5
11	120	6.8
12	150	9.65
13	160	9.05
14	180	9.20
15	210	8.6

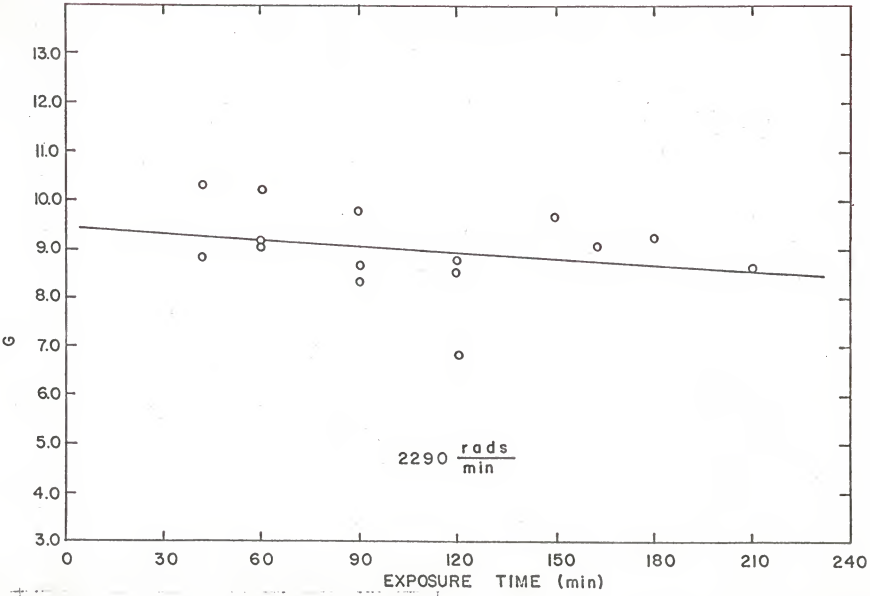

Fig. 20 Effect of absorbed dose on G.

constant. Above 50,000 rads there is a sudden decrease in the slope of the yield vs. absorbed dose plot. The relation holding above 50,000 rads is

$$y = K_2 + K_3 D. \tag{33}$$

This decrease in slope has been attributed to the consumption of all the dissolved oxygen in the solution (11). Since G is proportional to y/D, equation (33) yields a decreasing function of the form,

$$G = K_4 + K_5/D. \tag{34}$$

The negative slope found in the least squares analysis of the Mo(V) results could be attributed to a similar phenomenon producing a decreasing G function. Because of the lack of sufficient sensitivity in the methods of analysis available, an investigation could not be made in the region below 60,000 rads to determine any change in the slope of the yield vs. absorbed dose line.

However, as the 95 per cent variance of the slope was greater than the slope itself, it is impossible to state that the slope is definitely negative. Since the slope as determined above is small, it can be assumed that the G value is a constant in the range from 60,000 to 460,000 rads. From this point of view the most reasonable G value is the least squares or the mean value of 8.98 ± 0.92 ions oxidized/100ev. where 0.92 is the standard deviation.

C. Effect of Mo(V) Concentration on Mo(VI) Yields and the G Value. The G values obtained are tabulated with the Mo(VI) concentrations in Table 17. Figure 21 shows the least squares line of this data which can be represented by,

$$G = 8.364 + 23.7N, \qquad (35)$$

where N is the Mo(V) normality. The 95 per cent confidence limits on the slope result in a slope of 23.7 ± 118. As in the above section the variance is larger than the slope itself, making it impossible to definitely define the trend. By the same reasoning as above, it is possible to consider the G value as a constant within this Mo(V) concentration range The most reasonable G value is 8.82 ± 1.62. The larger standard deviation in this case resulted from shorter irradiation time. This independence of G on Mo(V) concentration was expected on theoretical grounds since in dilute solutions such as those investigated the photon interaction with the Mo(V) ions would be negligible, and almost all of the photon interactions take place in the solvent.

D. Effect of Hydrochloric Acid Concentration on the G Value. The G value was determined in aqueous solutions of Mo(V) varying from 0.3 to 4.0N in HCl. The data and G values obtained are shown in Table 18. The least squares line applying to the data is shown in Fig. 22 and can be represented by

$$G = 7.11 + 0.38N \text{ ions oxidized/100ev.} \qquad (36)$$

where N is the acid normality. The 95 per cent confidence

Table 17. Effect of Mo(V) concentration on G.

Sample number	10^3 x Mo(V)N	G
	moles/liter	ions oxidized/100ev.
1	0.91	10.40
2	1.10	10.10
3	2.60	10.30
4	2.60	9.65
5	2.60	9.43
6	2.60	8.98
7	3.51	9.07
8	3.73	8.32
9	4.21	7.83
10	5.40	10.90
11	5.40	8.40
12	5.62	10.7
13	5.62	10.6
14	5.62	10.4
15	5.62	8.25
16	5.50	8.07
17	5.60	8.27
18	6.80	7.76
19	6.80	7.52
20	6.80	7.34
21	6.80	7.18
22	6.80	6.85
23	7.20	9.95
24	7.50	12.40
25	7.50	12.0
26	7.81	9.3
27	7.81	8.82
28	7.81	6.03
29	7.81	5.72
30	16.3	7.10
31	19.0	11.2
32	19.2	7.5
33	22.0	7.2
34	26.0	9.13
35	26.0	8.58
36	32.0	8.66
37	10.8	7.80
38	13.1	8.75

Table 18. Data and calculated G values for irradiated Mo(V) solutions in various acidities. The irradiations were for 60 minutes and the ceric was 0.0072N.

Acidity	Ceric decrease	Mo(V) absorbance decrease	Fe(III) absorbance increase in 5 minutes	G by titration	G spectrophotometric
moles/liter	ml.	absorbance units	absorbance units	Mo(V) ions oxidized/ 100ev.	Mo(V) ions oxidized/ 100ev.
1.0N HCl	0.93±0.10	0.075±0.010	0.495±0.010	8.02±0.81	7.82±1.04
1.5N HCl	0.88	0.062	0.515	7.53±0.86	6.35±1.07
2.0N HCl	0.96	0.088	0.485	8.44±0.88	8.40±0.95
2.5N HCl	0.87	0.077	0.515	7.62±0.88	7.23±0.95
3.0N HCl	0.95	0.094	0.490	8.24±0.87	8.00±0.96
0.3N H_2SO_4: 0.3N HCl	0.69		0.228	12.5 ±1.8	
1.5N H_2SO_4: 0.3N HCl	0.63		0.228	11.4 ±1.8	
3.6N H_2SO_4: 0.3N HCl	0.67		0.228	12.1 ±1.8	

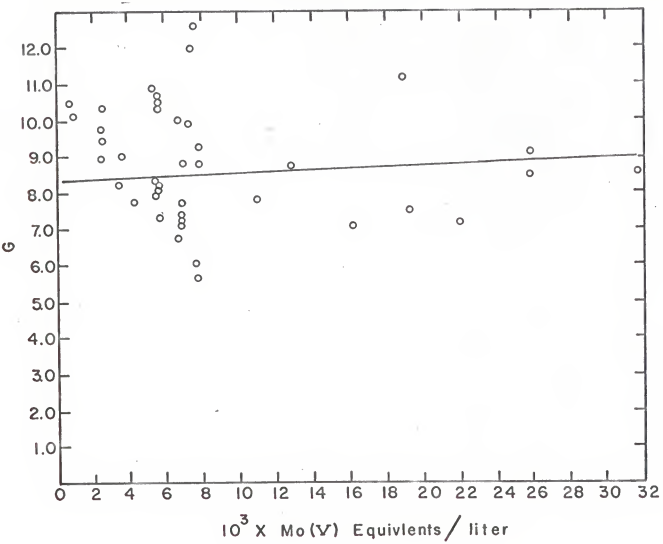

Fig. 21 Effect of Mo(V) normality on G.

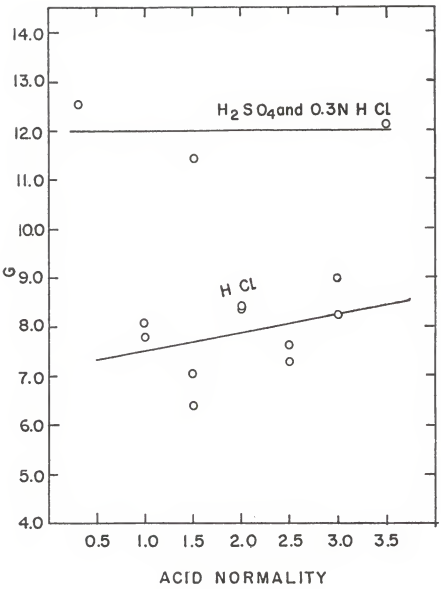

Fig.22 Effect of acidity on G.

limits of the slope are ±0.74 which makes it difficult to define a definite trend. The mean value and standard deviation are 7.87 and ±0.77 ions oxidized/100ev.

If the Mo(V) system is similar to the Fe(II) system, it is probable that the G value is more or less constant in this higher range of acidity. An investigation at lower acidity was not feasible because the Mo(V) becomes increasingly unstable as the acidity is reduced.

Figure 22 and Table 18 also include some G values of the Mo(V)-Mo(VI) system in mixture of HCl and H_2SO_4. The G value of the samples in the acid mixtures were found to be greater than those obtained in HCl alone. Schwarz and Hritz (24) observed a similar decrease in the yield of Fe(III) in HCl solutions of $FeCl_2$. They suggested that at high doses the Fe(III) chloride complexes competed effectively with oxygen for H atoms. In this investigation it was not possible to irradiate Mo(V) samples in H_2SO_4 alone as the only available methods for quantitatively reducing Mo(VI) to Mo(V) called for making the reduction in 3N HCl.

E. Effect of Degassing on the G Value. Samples of Mo(V) were degassed before irradiation as described in the experimental. The degassed samples were compared with the Mo(VI) yields of identical samples irradiated without degassing. The G values of the degassed samples were consistently lower. The ratios of the G values are tabulated as a function of Mo(V) concentration in Table 19 and are plotted against Mo(V) normality

Table 19. Data and ratios of G values for evacuated to unevacuated irradiated Mo(V) samples.

10^3 x Mo(V) normality	Acidity	Ceric decrease evacuated	Ceric decrease not evacuated	Absorbance decrease evacuated	Absorbance decrease not evacuated	G evac/ G not evac spectrophotometric	G evac/ G not evac titration
moles/ liter	moles/ liter	ml.	ml.	absorbance units	absorbance units		
3.16	2.0N HCl	0.72±0.10	0.84±0.10	0.026±0.010	0.035±0.010	0.742	0.855
4.20	2.0N HCl	0.42	0.74	0.019	0.028	0.678	0.568
5.60	2.0N HCl	0.32	0.47	0.025	0.031	0.807	0.681
7.51	2.0N HCl	0.50	0.63	0.024	0.025	0.961	0.894
9.36	2.0N HCl	0.52	0.62	0.015	0.018	0.833	0.840
11.80	0.3N H_2SO_4: 0.3N HCl	0.43	0.69				0.623
11.80	1.5N H_2SO_4: 0.3N HCl	0.51	0.63				0.808
11.80	3.6N H_2SO_4: 0.3N HCl	0.55	0.67				0.824

in Fig. 23. The least squares line of these data can be represented by

$$G_{evac}/G_{not\ evac} = 0.791 - 2.42N, \qquad (37)$$

where N is the Mo(V) normality. The 95 per cent confidence limits on the slope are ±6.30. The slope is small and the ratio of the G values may be given as 0.765±0.14 where ±0.14 is the standard deviation. These results indicate that the oxygen deficiency in the degassed solutions depressed the yield.

F. Limitations. As seen above the G value of the system under investigation had a relatively large variance. A major source of this variance, in the author's opinion, was the uncertainty in determining the irradiation yields. Because of the lack of a method for direct determination of small amounts of Mo(VI) in the presence of Mo(V), the yields were determined indirectly by measurement of the Mo(V) content before and after irradiation either spectrophotometrically or by titration.

As to titration, the volume difference in titrant for a 10 ml. sample before and after irradiation ranged from 0.20 to 0.90 ml. depending on the conditions of the irradiation. As the experimental accuracy in each titration was ±0.05 ml, each volume difference had a possible accumulative error of ±0.10 ml. Thus the possible experimental error in the Mo(VI) determinations ranged from 10 per cent to 50 per cent. This error could be reduced by irradiation to higher doses or by irradiation of larger samples. Irradiation dose in this study

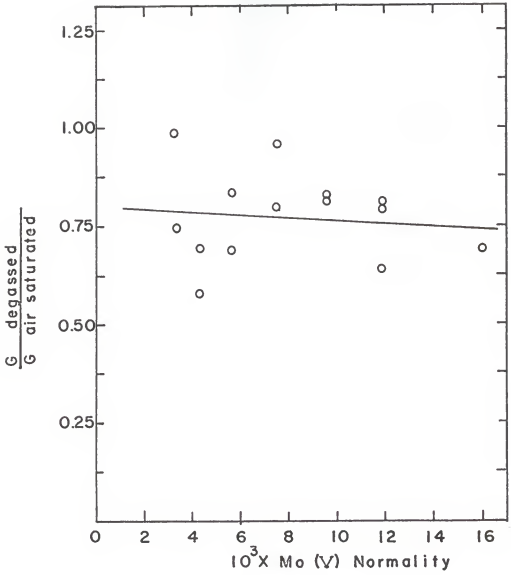

Fig. 23 Effect of degassing on G at varying Mo (V) N.

was limited by the limitations on the use of the X-ray machine. Use of larger samples would have subjected the sample to an inhomogeneous X-ray energy flux. The titrant, ceric sulfate, concentration could not be reduced as at lower concentrations the endpoints became vague.

Each absorbance measurement in the spectrophotometric analysis of Mo(V) had a possible experimental error or ±0.005. As the range of the absorbance decrease for the irradiated samples was from 0.015 to 0.080, the spectrophotometric analyses were subject to as large or larger possible experimental errors. This inconvenience in the spectrophotometry of the molybdenum system as compared to the iron system results from the fact that the sensitivity in the Fe(III) case is much larger. While the rate of change of absorbance with Mo(V) concentration is

$$(dA/dC)_{Mo(V)} = 63 \text{ abs. units/normality unit,} \quad (38)$$

it is 2300 in the Fe(III) case.

G. Conclusion. As suggested in section A, the overall effect of X-ray radiation on Mo(V) solutions is the partial oxidation to Mo(VI) as follows:

$$Mo(V) \xrightarrow{\text{radiation}} Mo(VI). \quad (39)$$

Since the solutions irradiated were very dilute in Mo(V), the reaction proceeds through a combination of reactions with the radiation decomposition products of water rather than by the direct oxidation of Mo(V) to Mo(VI). The formation of the radiation decomposition products of water is believed to take

place as follows:

$$H_2O \xrightarrow{\text{radiation}} H + OH \qquad (40)$$

$$OH + OH \text{ ----- } H_2O_2. \qquad (41)$$

The reactions of these products with molybdenum ions may be represented by

$$Mo(V) + OH \text{ ----- } Mo(VI) + OH^-, \qquad (42)$$

$$Mo(VI) + H \text{ ----- } Mo(V) + H^+, \qquad (43)$$

and $$Mo(V) + H_2O_2 \text{ ----- } Mo(VI) + OH^- + OH. \qquad (44)$$

The results of section C showed that the initial Mo(V) concentration had little or no effect on the Mo(VI) yields or the G value in the concentration range from 1×10^{-3} to 30×10^{-3} milliequivalents Mo(V)/ml. Had the observed oxidation been a result of a direct photon interaction with the Mo(V) ions, the G value would have increased as the Mo(V) concentration increased.

As the yield and thus the G value was 1.3 times greater in samples exposed to air than in degassed samples, the dissolved oxygen in the non-degassed samples must have promoted the oxidation. The increased oxidation from dissolved oxygen probably proceeds by the reactions

$$H + O_2 \text{ ----- } HO_2, \qquad (45)$$

$$HO_2 + Mo(V) \text{ ----- } Mo(VI) + HO_2^-, \qquad (46)$$

and $$HO_2^- + H^+ \text{ ----- } H_2O_2. \qquad (47)$$

The HO_2 radical is seen to be capable of causing two oxidations in acid media.

Neither the HCl nor the H_2SO_4 concentration was observed

to appreciably affect the G value of the system in the range from 0.3 to 3.5N acid. Reactions (43) and (47) indicate that the oxidation would increase with increasing acid concentration by the common ion effect. However, in the high range of acidity of the samples investigated, this effect would already have reached a saturation level. The G value of the Mo(V)-Mo(VI) system was observed to be higher in mixtures of H_2SO_4 and HCl than in HCl alone. This may be explained by the fact that the Mo(VI) complexes compete effectively with oxygen for H atoms in a manner analogous to Fe(III) chloride complexes (24).

The G value was affected very lightly by total absorbed dose in the range from 60,000 to 460,000 rads which made it feasible to consider the G value as 8.98 ± 0.81 for Mo(V) solutions in HCl.

Using the widest limits of the G values and their standard deviations as calculated from varying absorbed dose between 60,000 and 460,000 rads, varying Mo(V) concentration between 1×10^{-3} and 30×10^{-3}N and varying HCl normality from 1 to 3N, an overall G value within these limits may be represented as 8.26 ± 2.14. As this G value covers such a wide range, it cannot be expected that the Mo(V)-Mo(VI) system could be used to measure absorbed dose to a high degree of accuracy. The use of a more accurate method of determining Mo(VI) yields could very well allow a more precise representation of this G value. Also the G value could have been more accurately defined

for the type of analyses used, had it been possible to subject the samples to a larger absorbed dose.

SUGGESTIONS FOR FURTHER WORK

As indicated in the discussion, the biggest drawback of the investigation of the effects of X-ray irradiation on Mo(V) samples was the lack of a highly sensitive method of analysis for the irradiation yields. A direct spectrophotometric analysis for the Mo(VI) formed in the presence of Mo(V) would be ideal. Recently Majumdar and Savarian (18), and Busev and Chan (1) have published papers on very sensitive analytical methods for direct determination of Mo(VI). As neither author has commented on the effect of Mo(V) present, it would be of interest to test the applicability of these analyses in the presence of Mo(V).

It would be desirable to investigate the radiation induced oxidation of Mo(V) to Mo(VI) in the range below a 60,000 rads total absorbed dose. A more sensitive method of analysis for the Mo(VI) yields than those employed in this thesis would be necessary. An investigation in this range would show whether or not there is a breaking point in the Mo(VI) yield line as a function of total absorbed dose.

The analyses employed in this thesis would be more applicable in investigations where the Mo(VI) yields were an order of magnitude higher. Providing that the G value remains relatively constant as the dose increases, total absorbed doses

in the range of a million rads would give these higher yields. This type of dosage could be obtained if the samples were subjected to the gamma flux of a nuclear reactor. Also the gamma flux of a reactor would allow a study to be made of the effect of radiation intensity on the G value.

The effect of photon energy on the G value of the Mo(V)-Mo(VI) system might be investigated using monoenergetic sources such as cobalt 60. It would be of interest to investigate the effect of different types of radiation such as beta and alpha particles on the Mo(V)-Mo(VI) system.

An investigation into the effects of radiation on Mo(III) and Mo(IV) could be made. Also a study of the effect of dissolved scavengers on the irradiation yields would be of interest.

An extenuation of the study of Mo(V) stability at different temperatures to a wide range of initial Mo(V) concentrations and a wide range of solvent concentrations may allow some conclusion to be made as to the exact form of the reaction taking place.

ACKNOWLEDGMENT

The author wishes to express his appreciation to the Kansas State University Engineering Experiment Station for their financial support in making this project possible. Sincere gratitude is given to Dr. S. Z. Mikhail for his advice, guidance, and encouragement throughout this study. Thanks are also extended to Dr. J. O. Mingle of the Kansas State Nuclear Engineering Staff for his particular contribution and to the other staff members and the graduate students for their willingness to assist when called upon.

LITERATURE CITED

1. Busev, A. I., and F. Chan
   Direct Complexometric Determination of Sexivalent Molybdenum. Vestnik Moskov. Univ., Ser. Mat., Mekh. Astron., Fiz. i Khim 14, No. 2203. 1959.

2. Clark, G. L.
   Applied X-rays. New York: McGraw Hill, 1955.

3. Dewhurst, H. A., A. H. Samuel and J. L. Magee.
   Theory of Radiolysis of Water. Rad. Res. 1, 73. 1954.

4. Dyne, P. J., and J. M. Kennedy.
   Can. J. Chem. 36, 1518. 1958

5. Dyne, P. J., and J. M. Kennedy.
   Can J. Chem. 38, 61. 1960.

6. Flanders, D. A., and H. Fricke.
   J. Chem. Phys. 28. 1126. 1958.

7. Fricke, H.
   Ann. N. Y. Acad. Sci. 59, 567. 1955.

8. Furman, N. H., and W. M. Murray.
   Studies of the Reducing Action of Mercury II.
   J. Am. Chem. Soc. 58, 1689. 1936.

9. Harlan, J. T., and E. J. Hart.
   Ceric Dosimetry: Accurate Measurements at 10^8 Rads.
   Nucleonics. 17(8): 102. 1959.

10. Hart, E. J.
    Chemical Dosimetry. Argonne National Laboratory, Lemont, Illinois.

11. Hart, E. J.
    Development of the Radiation Chemistry of Aqueous Solutions. J. of Chem. Ed. 36(6): 266. 1959.

12. Hiskey, C. F., and V. W. Meloche.
    The Nature of the Thiocyanate Complex of Molybdenum.
    Am. Chem. Soc. J. 62, 1566. 1940.

13. Hiskey, C. F., and V. W. Meloche.
    Phenomena Associated with Quinquevalent Molybdenum Solutions. J. Am. Chem. Soc. 62, 1819. 1940.

14. Kupperman, A., and G. G. Belford.
Diffusion Kinetics in Radiation Chem. Noyes Chemical Lab., University of Illinois, Urbana, TID-6456, 1960.

15. Kupperman, A.
Diffusion Kinetics. Nucleonics. 19(10): 38. 1961.

16. Lea, D. E.
Brit. J. Radiol. Suppl. 1, 59. 1947.

17. Magee J. L.,
J. chim. phys. 52, 528. 1955.

18. Majumdar, A. K., and C. P. Savariar.
Spectrophotometric Determination of Mo with 9-Methyl-2, 3, 7-Trihydroxy-6 Flurone. Anal. Chim. Acta. 22, 158. 1960.

19. McCarthy, P. J.
Introduction to Statistical Reasoning. New York: McGraw Hill. 1957.

20. Price, W. J.
Nuclear Radiation Detection. New York: McGraw Hill, 1958.

21. Rao, G. G., and M. Z. Suryanarayana.
Oxidimetric Methods for the Volumetric Determination of Molybdenum (V). Z. anal. Chem. 169, 160. 1959.

22. Riggs, T., G. Stein and J. Weiss
The Action of X-rays on Ferrous and Ferric Salts in Aqueous Solutions. Roy. Soc. of Lond. 211, 375. 1952.

23. Samuel, A. H., and J. L. Magee.
J. Chem. Phys. 21, 1080. 1953.

24. Schwarz, H. A., and J. M. Hritz.
The Radiation Chemistry of Deaerated Ferrous Chloride Systems. J. Am. Chem. Soc. 80(11): 5636. 1958.

25. Schwarz, H. A.
J. Am. Chem. Soc. 77, 4960. 1955.

26. Scott, W. W.
Standard Methods of Chemical Analysis. New York: Van Nostrand, 1939.

27. Stein, G., and J. Weiss.
J. Chem. Soc., 3354. 1949.

28. Stein, G., R. Watt and J. Weiss.
The Reduction of Mercuric Chloride in Aqueous Solutions by X-rays. Nature. 1030. 1952.

29. Willard, H. H., and P. Young.
Ceric Sulfate as a Volumetric Oxidizing Agent. Am. Chem. Soc. J. 50, 1322. 1928.

30. Wylie, C. R.
Advanced Engineering Mathematics. New York: McGraw Hill, 1960.

APPENDICES

APPENDIX A

Free Radical Formation in Water

Hart (19) has suggested a mechanism for the production of free radicals in water. A brief summary of his views follows.

X-rays and gamma rays eject photo- and/or Compton recoil electrons from gas molecules. It is postulated that these electrons are also formed in water and produce multiple ionizations in it. These ions and electrons are converted into free radicals by the following reactions:

$$H_2O + e_c = H_2O^+ + e_{c1} + e_s \qquad \text{(A-1)}$$

$$H_2O + e_{cn} = H_2O^+ + e_{c,n+1} + e_s$$

$$H_2O + e_s = H_2O^+ + e_{s1} + e_s \qquad \text{(A-2)}$$

$$H_2O + e_s = H_2O^+ + e_{s,n+1} + e_s$$

$$H_2O^+ + H_2O = H_3O^+(aq) + OH \qquad \text{(A-3)}$$

$$H_2O + (e_s \text{ or } e_{sn}) = H + OH^-(aq) \qquad \text{(A-4)}$$

where e_c = recoil electron, e_{cn} = recoil electron after the nth ionization, e_s = secondary electron, e_{sn} = secondary electron after the nth ionization.

Reaction (A-1) is the primary ionization process initiated by a recoil electron (e_c). Secondary electrons (e_s) and the original slightly degraded recoil electron (e_{c1}) continue the ionization processes represented by reactions (A-2). Depending on the velocity of the ionizing particle, these ionization processes require of the order of 10^{-16} to

10^{-18} sec. (10). The conversion of H_2O^+ into a hydroxyl radical (reaction A-3) requires about 10^{-11} sec., the time of dielectric relaxation and orientation of dipoles. The thermalization and capture of electrons (reaction A-4) forming a hydrogen atom also requires a time of this order of magnitude. The result of these ionization processes is a net dissociation of the water molecule as follows:

$$H_2O \xrightarrow{\text{radiation}} H + OH \qquad \text{(A-5)}$$

APPENDIX B

Derivation of the Absorbance Equation

Experimentally it was found that

$$dA/dC = a_1 + a_2T, \tag{B-1}$$

and that

$$dA/dT = a_3 + a_4C. \tag{B-2}$$

C and T can be called independent variables as there is no change in temperature as the concentration is varied and vice versa. Actually some dependence exists between these variables but it is negligible being in the form of the heat of solution and the temperature dependence of the density. Considering A as a function of the independent variables C and T, equations (B-1) and (B-2) may be solved in the following manner.

Let $A = f(C,T)$. (B-3)

Then $dA/dC = df(C,T)/dC$ (B-4)

and $dA/dT = df(C,T)/dT$. (B-5)

$$dA = df(C,T) = \frac{\partial f}{\partial T}(C,T)dT + \frac{\partial f}{\partial C}(C,T)dC. \tag{B-6}$$

Thus $$\frac{dA}{dT} = \frac{df}{dT}(C,T) = \frac{\partial f}{\partial T}(C,T) + \frac{\partial f}{\partial C}\frac{dC}{dT}^{0} \tag{B-7}$$

and $$\frac{dA}{dC} = \frac{df}{dC}(C,T) = \frac{\partial f}{\partial T}(C,T)\frac{dT}{dC}^{0} + \frac{\partial f}{\partial C}(C,T). \tag{B-8}$$

Then substitute (B-1) and (B-2) into (B-6) using (B-7) and (B-8) to get

$$df(C,T) = (a_1 + a_2T)dC + (a_3 + a_4C)dT \tag{B-9}$$

which integrates directly into

$$A = f(C,T) = K_0 + K_1C + K_2T + K_3CT. \qquad \text{(B-10)}$$

APPENDIX C

Least Squares Solution of the Absorbance Equation

N sets of data relating A to C and T were applied to the equation

$$A_i = K_0 + K_1C_1 + K_2T_1 + K_3C_1T_1. \qquad \text{(C-1)}$$

In matrix notation this can be represented by

$$\begin{pmatrix} 1 & C_1 & T_1 & C_1T_1 \\ \cdot & \cdot & \cdot & \cdot \\ \cdot & \cdot & \cdot & \cdot \\ \cdot & \cdot & \cdot & \cdot \\ 1 & C_i & T_i & C_iT_i \\ \cdot & \cdot & \cdot & \cdot \\ \cdot & \cdot & \cdot & \cdot \\ \cdot & \cdot & \cdot & \cdot \\ 1 & C_n & T_n & C_nT_n \end{pmatrix} \begin{Bmatrix} K_0 \\ K_1 \\ K_2 \\ K_3 \end{Bmatrix} = \begin{pmatrix} A_1 \\ \cdot \\ \cdot \\ \cdot \\ A_i \\ \cdot \\ \cdot \\ \cdot \\ A_n \end{pmatrix} . \qquad \text{(C-2)}$$

Pre-multiplying both sides through by the inverse of the coefficient matrix results in the matrix equation,

(C-3)

$$\begin{pmatrix} \sum N & \sum C_i & \sum T_i & \sum C_iT_i \\ \sum C_i & \sum C_i^2 & \sum T_iC_i & \sum C_i^2T_i \\ \sum T_i & \sum C_iT_i & \sum T_i^2 & \sum C_iT_i^2 \\ \sum C_iT_i & \sum C_i^2T_i & \sum T_i^2C_i & \sum C_i^2T_i^2 \end{pmatrix} \begin{Bmatrix} K_0 \\ K_1 \\ K_2 \\ K_3 \end{Bmatrix} = \begin{Bmatrix} \sum A_i \\ \sum C_iA_i \\ \sum T_iA_i \\ \sum C_iT_iA_i \end{Bmatrix},$$

where $\sum$ represents the summation over the i sets of data. This is equivalent to a set of simultaneous equations and may be solved as such. This set of simultaneous equations was solved on the IBM 650 computer using a modified Crout reduction program, the flow sheet of which follows.

Flow diagram for least squares solution of absorbance equation.

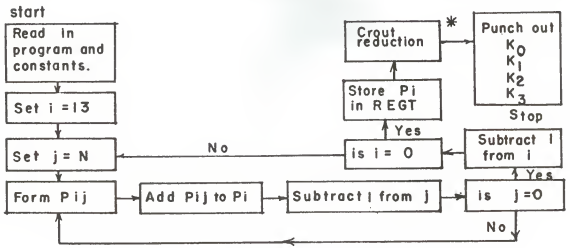

The following symbology is used

Pij equals : I , when i equals: I
C_j	2
T_j	3
C_j T_j	4
A_j	5
C_j^2	6
C_j^2 T_j	7
C_j A_j	8
T_j^2	9
C_j T_j^2	10
T_j A_j	11
C_j^2 T^2	12
C_j T_j A_j	13

The subscript j refers to each of the individual I through N sets of data.

* The Crout reduction program was supplied by Dr. J. O. Mingle.

X-RAY IRRADIATION EFFECTS ON THE Mo(V)-Mo(VI) SYSTEM IN AQUEOUS MEDIA

by

DONALD FREDERICK PADDLEFORD

B. S., Kansas State University, 1960

AN ABSTRACT OF A MASTER'S THESIS

submitted in partial fulfillment of the

requirements for the degree

MASTER OF SCIENCE

Department of Nuclear Engineering

KANSAS STATE UNIVERSITY
Manhattan, Kansas

1962

The main purpose of this study was to determine the effect of X-ray radiation on molybdenum ions. Mo(V) solutions of different composition and acidity were irradiated and analyzed. The temperature of Mo(V) solutions was observed to increase during irradiation. This necessitated an investigation of the temperature dependence of the Mo(V) light absorbance because the samples were to be analyzed spectrophotometrically. This investigation was carried from room temperature to 55°C for solutions ranging from 1.2 to 4.0N in HCl at wavelengths from 350mμ to 450mμ. The results showed that it was possible to represent the temperature dependence of Mo(V) absorbance as a linear function of Mo(V) concentration, and to represent the Mo(V) concentration dependence of Mo(V) absorbance as a linear function of sample temperature. The equation resulting from the solution of these two linear differential equations was experimentally tested making use of the IBM 650 computer. Two methods of calculating the constants of the equation were investigated. It was found that calculated absorbances using this equation were in good agreement with those observed.

A study of the instability of Mo(V) due to autoxidation was made at temperatures from 30 to 60°C. It was found that the autoxidation corrections to the Mo(V) irradiation induced concentration changes were negligible under the irradiation conditions used.

The effect of X-ray irradiation on dilute solutions of

Mo(V) and Mo(VI) was investigated. Mo(V) in acid solution was found to undergo an oxidation to the Mo(VI) state on absorption of X-ray radiation. No chemical change was observed in irradiated samples of Mo(VI) indicating that the rate of reaction of Mo(V) with the oxidizing decomposition products of water occurred at a higher rate than did reactions of Mo(VI) with reducing decomposition products. Samples of Mo(V) were irradiated to various total absorbed doses in the range from 60,000 to 460,000 rads and the G value of the Mo(V) to Mo(VI) reaction in this range was found to be nearly constant. Irradiation of samples of varying Mo(V) concentration showed that the G value of the system had little or no concentration dependence from 1×10^{-3} to 30×10^{-3} milliequivalents Mo(V)/ml. From this it was concluded that the oxidation of the Mo(V) was the net result of the free radical reactions,

$$Mo(V) + OH \text{ ----- } Mo(VI) + OH^- \qquad (1)$$

$$Mo(VI) + H \text{ ----- } Mo(V) + H^+ \qquad (2)$$

$$Mo(V) + H_2O_2 \text{ ----- } Mo(VI) + OH^- + OH, \qquad (3)$$

rather than a result of direct oxidation of Mo(V) on absorption of X-rays.

Irradiation of degassed samples of Mo(V) showed that the oxidation of Mo(V) to Mo(VI) was depressed by a factor of about 0.77 in solutions containing no dissolved oxygen. The increased oxidation in the samples containing dissolved oxygen was concluded to proceed by the reactions,

$$H + O_2 \text{ ----- } HO_2 \quad (4)$$

$$Mo(V) + HO_2 \text{ ----- } Mo(VI) + HO_2^- \quad (5)$$

$$HO_2^- + H^+ \text{ ----- } H_2O_2, \quad (6)$$

where the H_2O_2 can oxidize Mo(V) as shown in reaction (3). In the range from 1 to 3N HCl the G value of the Mo(V)-Mo(VI) system was found to be nearly independent of the acid normality. This indicates that the common ion effect which caused an increase in G with increase in acidity had reached a saturation level. Irradiated Mo(V) solutions in mixtures of HCl and H_2SO_4 were found to have higher Mo(VI) yields and thus a larger G value than were exhibited in HCl solutions. The decreased yields in the HCl solutions may be explained by the fact that the Mo(VI) complexes compete effectively with oxygen for H atoms as do Fe(III) chloride complexes in HCl solutions.

Suggestions for further investigation on this system have been made particularly with respect to recent advances in the methods of analysis for Mo(VI).